

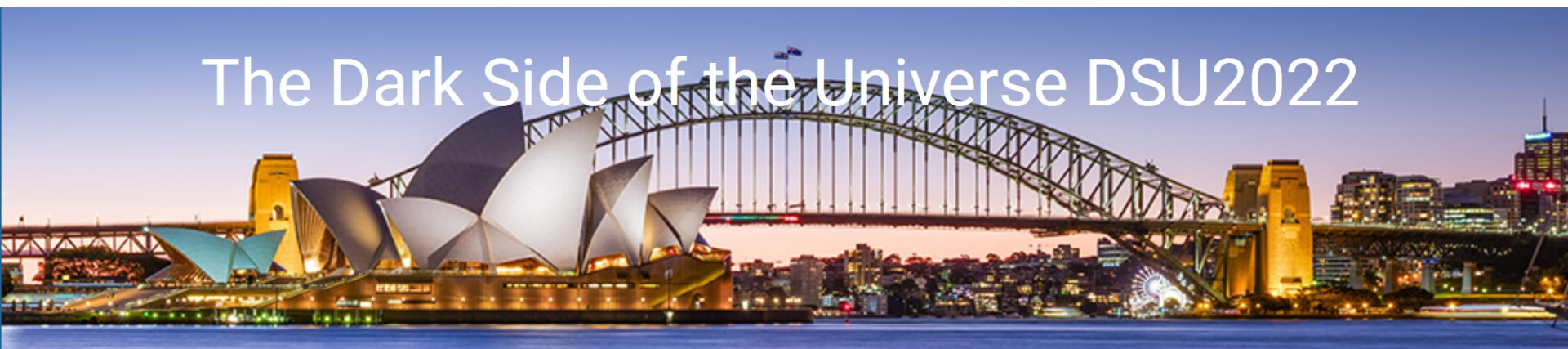
# Cosmic ray boosted dark matter

**Yu-Feng Zhou**

Institute of Theoretical Physics,  
Chinese Academy of Sciences

Yan-Hao Xu, Chen Xia, YFZ,  
arXiv:[2009.00353](https://arxiv.org/abs/2009.00353), arXiv:[2111.05559](https://arxiv.org/abs/2111.05559), arXiv:[2206.11454](https://arxiv.org/abs/2206.11454)

The Dark Side of the Universe DSU2022

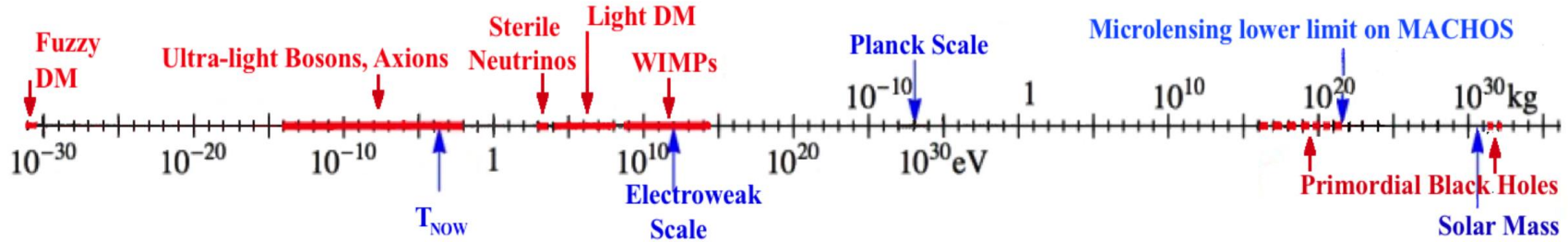


# Outline

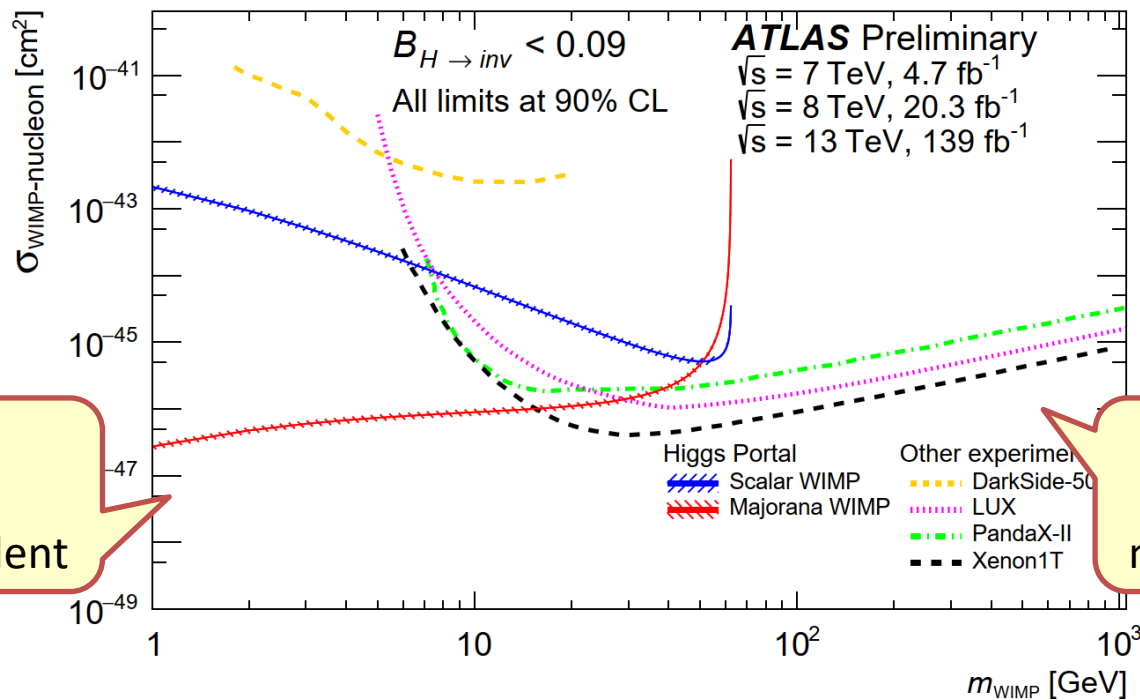
---

- Introduction: DM scattering in space
- CR boosted DM (CRDM) as a new probe for light DM
- Earth attenuation of CRDM
- Distinguishing CRDM from other boosted DM models
- Summary

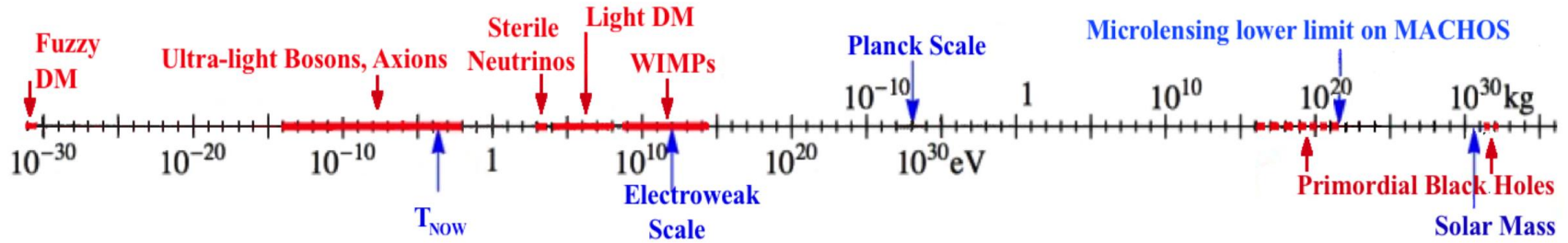
# Particle Dark Matter: mass, spin, interaction strength ?



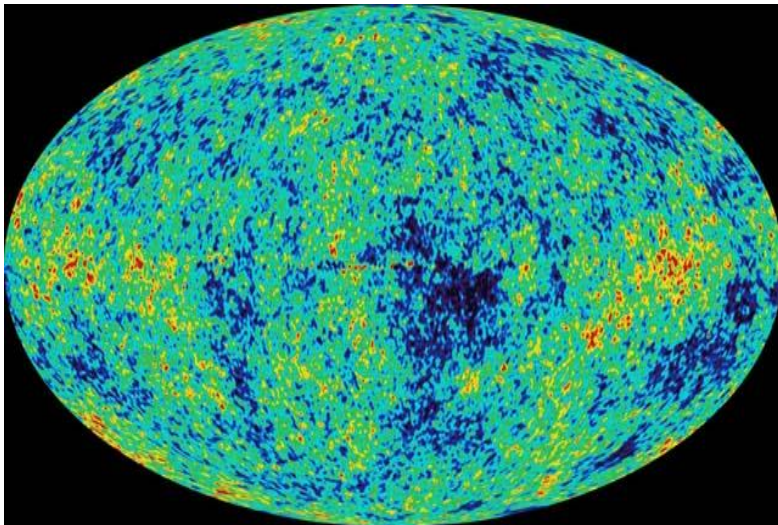
## Collider search vs Direct detection



# Particle Dark Matter: mass, spin, interaction strength ?

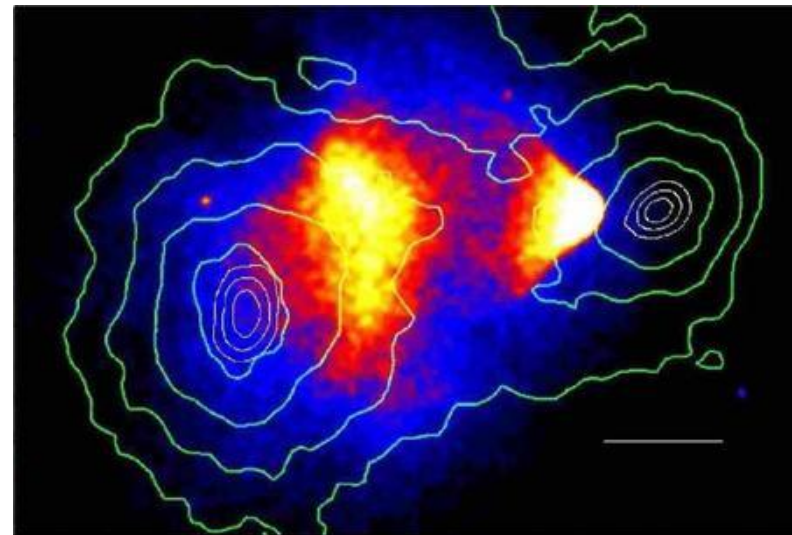


DM can collide with matter everywhere in space !



CMB:  $\sigma_{\chi N} < 10^{-27} \text{cm}^2 (m_{\chi} < \text{GeV})$

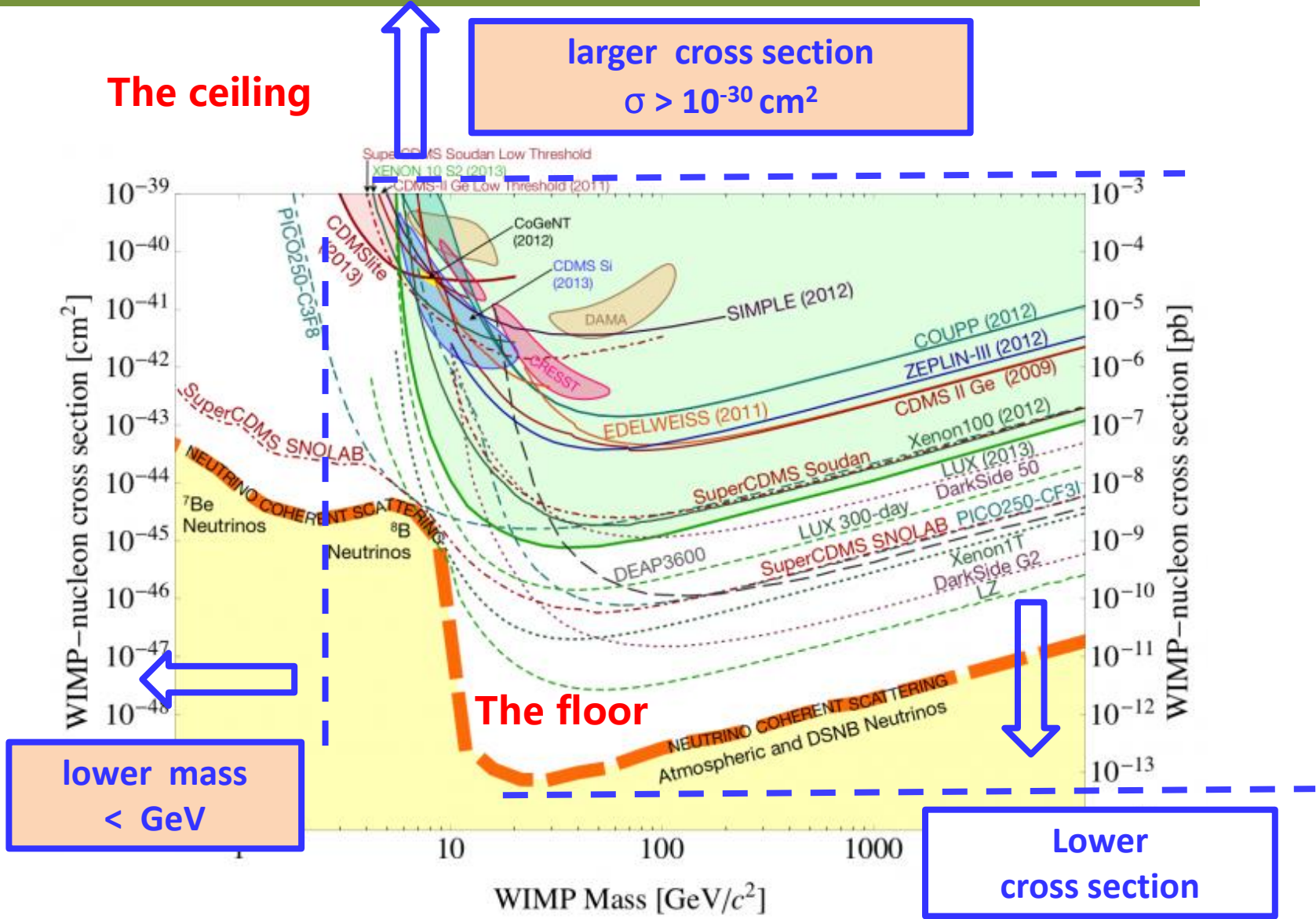
Gluscevic, Boddy, arXiv:1712.07133



1E0657-56:  $\sigma_{\chi N} / m_{\chi} < 1.7 \text{cm}^2 / \text{g}$

Kahlhoefer, et al (2014)

# Frontiers of DM direct searches



## Frontier 1: Low DM particle mass ( $< \text{GeV}$ )

- Nuclear recoil energy depends on halo DM mass and velocity distribution

$$E_R = \frac{2m_N}{(1 + m_\chi/m_N)^2} \left( \frac{m_\chi}{m_N} \right)^2 v_{\min}^2$$

Halo DM velocity is limited by the escape velocity  $v_{\text{esc}} \sim 500 \text{ km/s}$

$$f_{\text{halo}}(\mathbf{v}) = \frac{1}{N} \exp\left(-\frac{v^2}{v_0^2}\right) \Theta(v_{\text{esc}} - v),$$

### Difficulties in probing low mass DM

- low momentum of DM particles  $p_\chi \approx O(\text{MeV})(m_\chi/\text{GeV})$
- low energy transfer from elastic scattering process  $\left(\frac{m_\chi}{m_N}\right)^2$

For 1 GeV DM and 100 GeV target, the maximal recoil energy is  $\sim 0.06 \text{ keV}$

But the typical direct detection thresholds is  $O(\text{keV})$  !

# Frontier 2: large scattering cross section ( $>10^{-30} \text{ cm}^2$ )

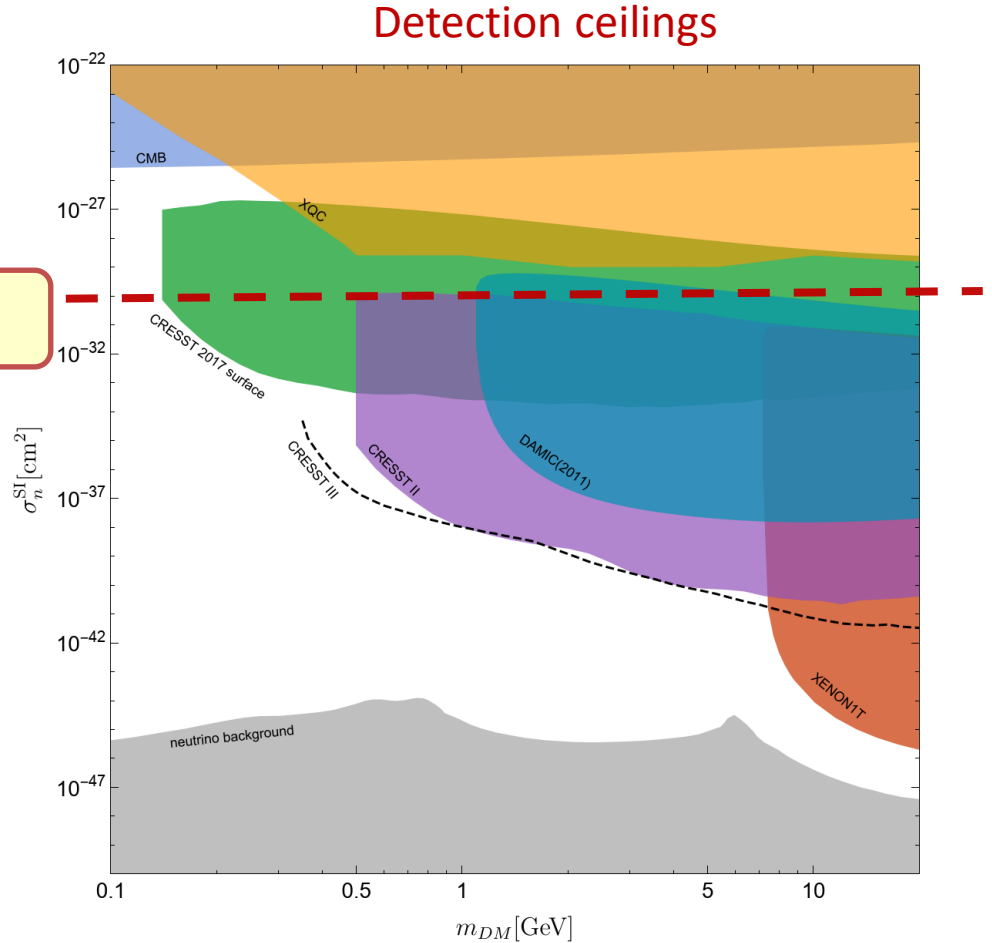
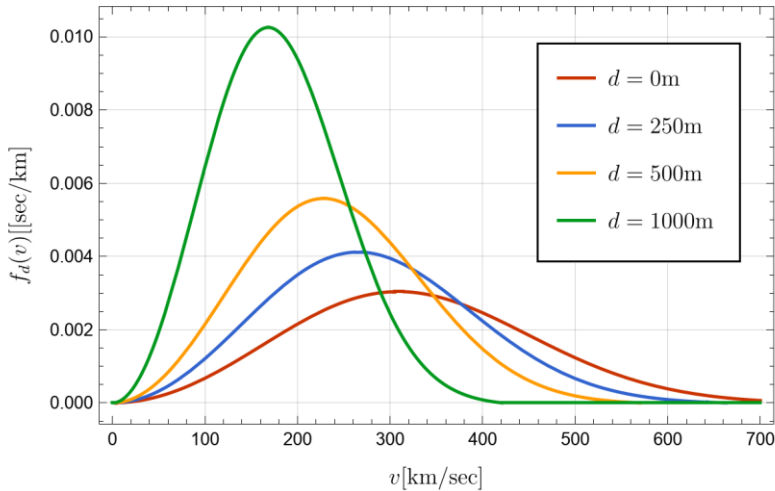
DM lose energy after penetrating the Earth's crust (non-relativistic case:  $dE/dz \approx E$ )

$$\frac{dE_\chi}{dx} = - \sum_i n_i \frac{2\mu_{\chi i}^2 \sigma_{\chi i}^{tot}}{m_i m_\chi} E_\chi,$$

A critical cross section appears due to the energy cutoff

O(1) factor

$$\sigma_{\chi n} = \frac{m_\chi \mu_{\chi n}^2}{2\rho d \sum_i \frac{f_i \mu_{\chi i}^4 A_i^2}{m_i^2}} \log \left( \frac{E_\chi^{ini}}{E_\chi^{min}} \right).$$



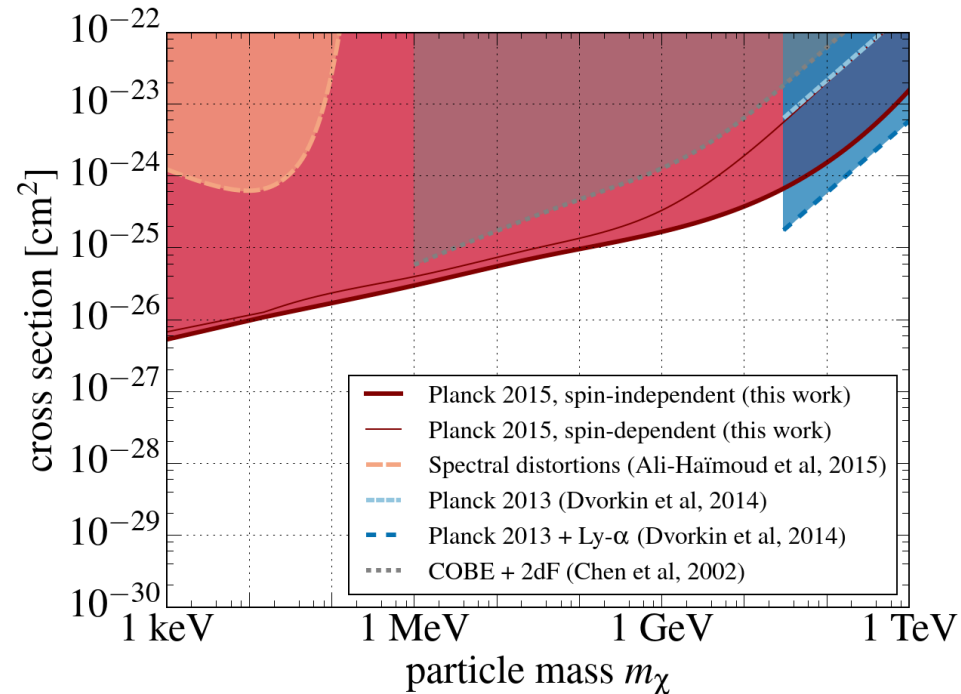
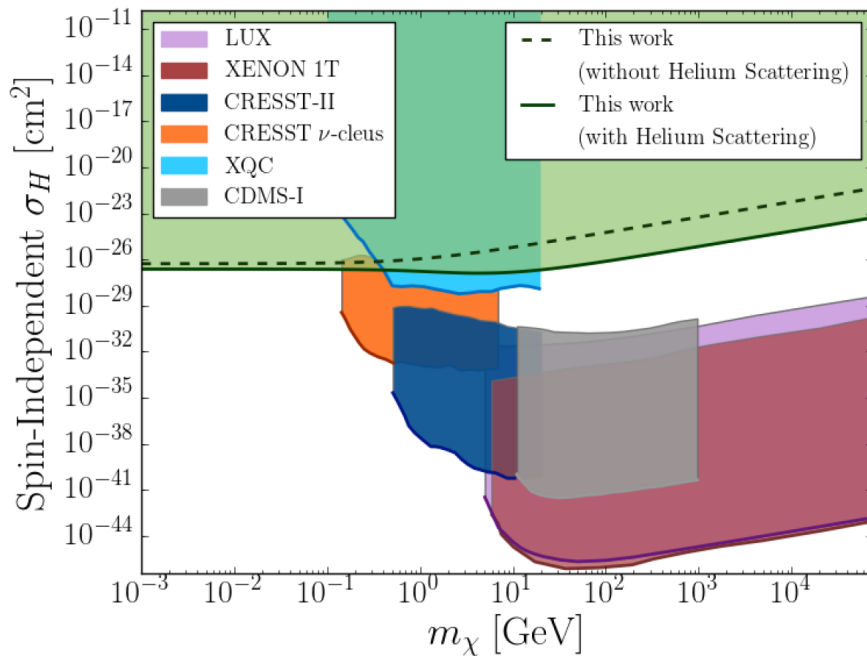
Emken & Kouvaris, arXiv:1802.04764

# DM scattering in space: CMB

## DM-proton scattering 380000 yrs after the Big Bang

- Distortion of CMB spectrum
- Suppression of small scale structure (drag force)

Constraints:  $\sigma < 10^{-27} \text{ cm}^2$  for  $m_\chi \ll \text{GeV}$



Constraints insensitive to DM particle mass

Gluscevic & Boddy, arXiv:1712.07133



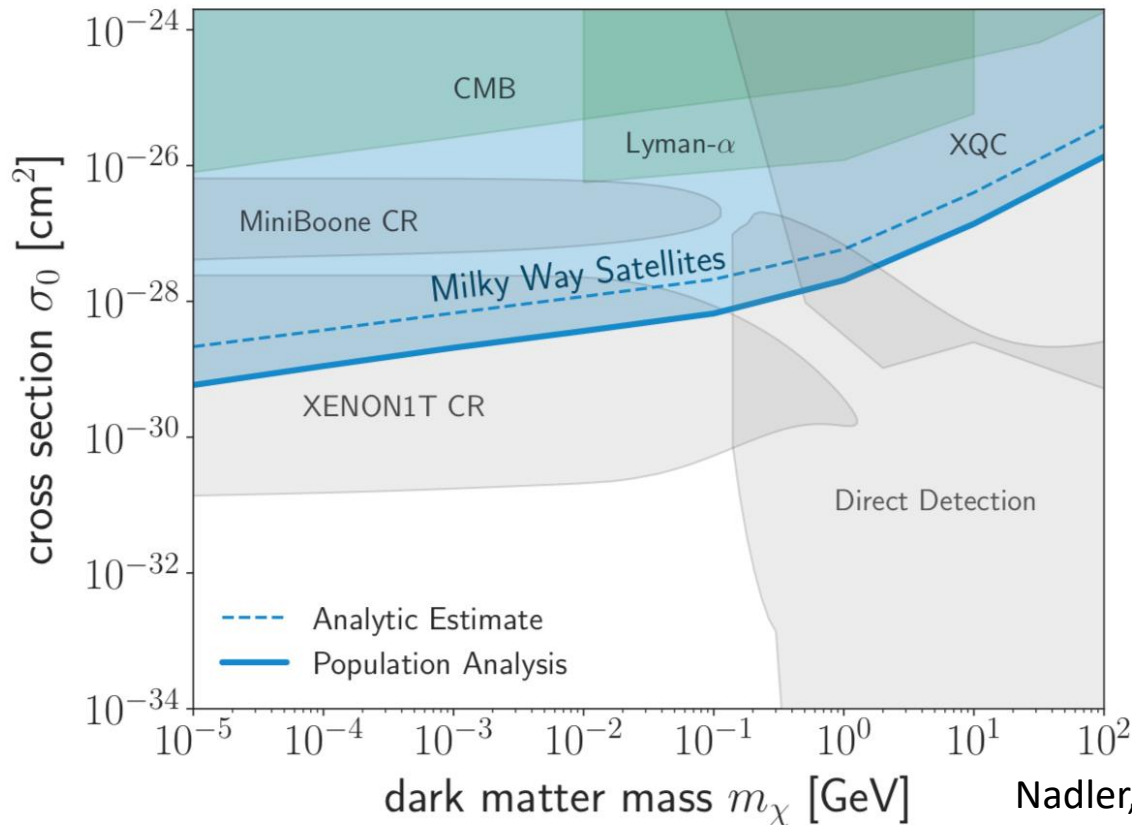
# DM scattering in space: structure formation

DM-proton scattering damp structure perturbation

Distribution of dwarf satellite galaxies is modified

$\sigma < 6 \times 10^{-30} \text{ cm}^2 @ 10 \text{ keV}$ , ( $< 10^{-27} \text{ cm}^2 @ 10 \text{ GeV}$ )

Upper limits scale with DM mass as  $m^{1/4}$  for  $m \ll 1 \text{ GeV}$



Nadler, et al., arXiv:1904.10000

DES, arXiv:2008.00022

Constraints insensitive to DM particle mass

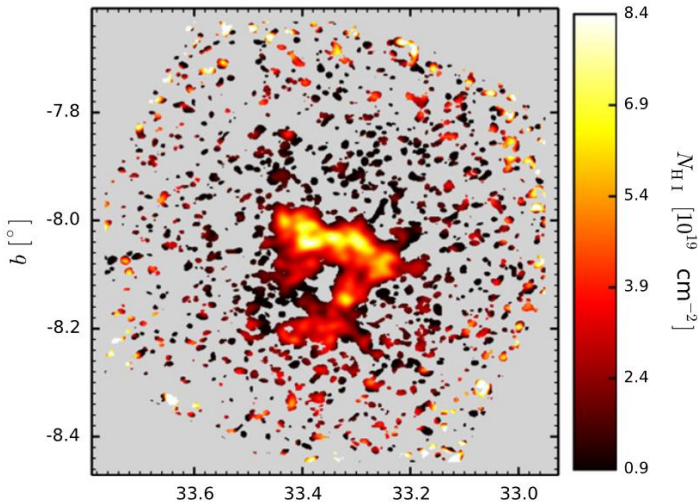
# DM scattering in space: gas cooling

DM above KeV has a temperature higher than the coldest atomic gas

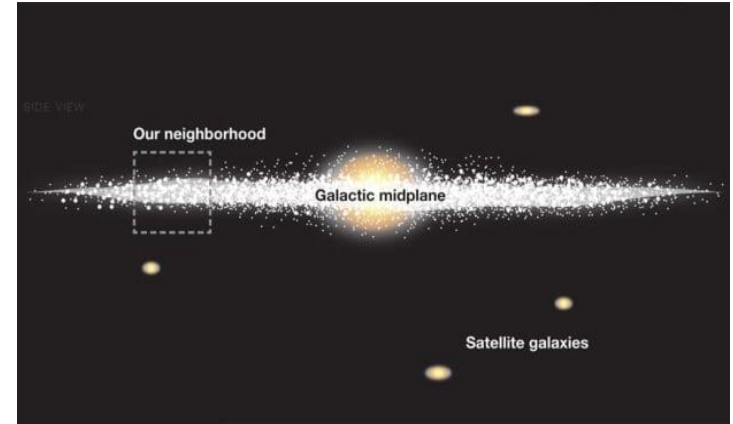
$$T_x \sim m_x v_x^2 \simeq 10^4 \text{ K} \left( \frac{m_x}{\text{MeV}} \right) \left( \frac{v_x}{10^{-3}} \right)^2,$$

DM-proton scattering heat the gas and change its cooling rate

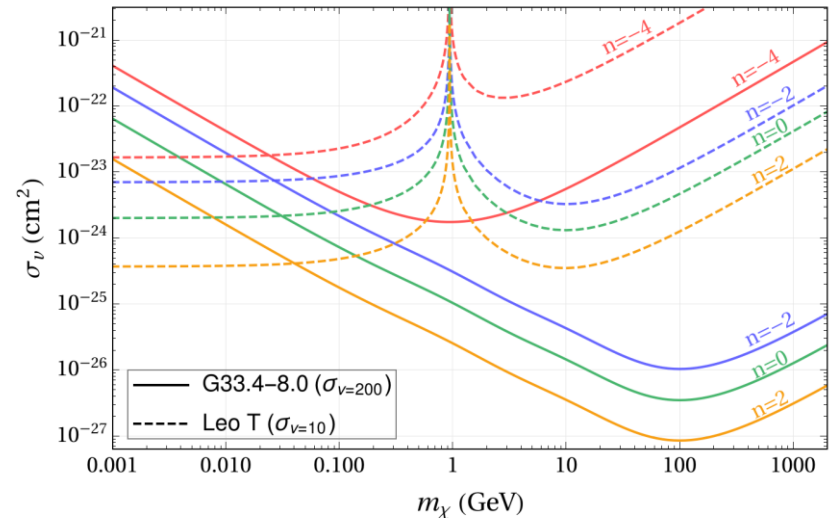
$\sigma < 10^{-(23-25)} \text{ cm}^2$  for a large mass range  
 $10^{-23} \text{ eV} \text{ -- } 10^{-10} \text{ eV}$  from dwarf galaxy Leo T



Gas cloud G33.4-8.0



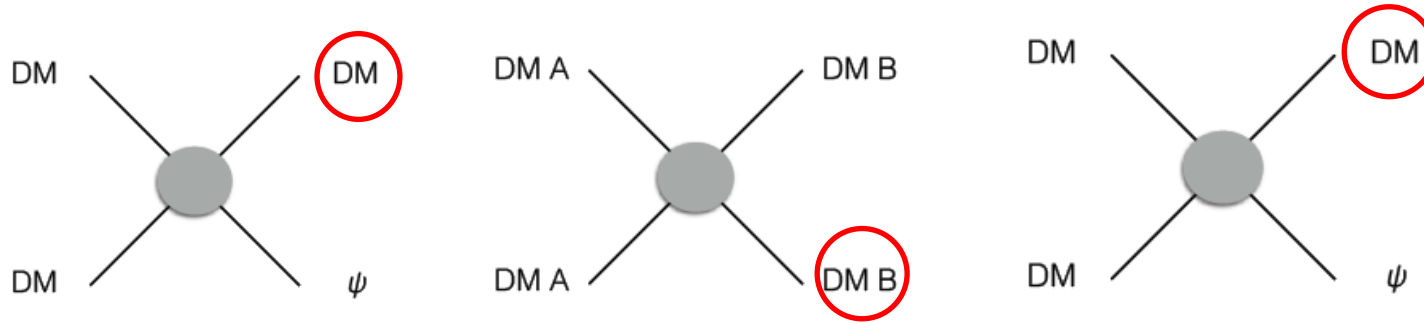
dwarf galaxies



Wadeker & Farrar, arXiv:1903.12190

# Beyond halo DM: boosted DM sub-components ?

## boosted DM subcomponents from dark sectors



### □ Decay $A \rightarrow \bar{B}B$

$$\left( \frac{d\Phi_\chi}{dT_B d\Omega} \right)_{\text{dec}} = \frac{1}{4\pi m_A \tau_A} \frac{dN}{dT_B} \int_{\text{l.o.s}} dl \rho_\chi(\mathbf{r}),$$

J. Berger, Y. Cui, Y. Zhao. JCAP, (2015)

- Energy spectra well-determined
- Known angular distributions

### □ Annihilation $\bar{A}A \rightarrow \bar{B}B$

$$\left( \frac{d\Phi_\chi}{dT_B d\Omega} \right)_{\text{ann}} = \frac{\langle \sigma_{\text{ann}} v \rangle}{8\pi m_A^2} \frac{dN}{dT_B} \int_{\text{l.o.s}} dl \rho_\chi^2(\mathbf{r}),$$

### □ 3→2 Semi-annihilation

$$\left( \frac{d\Phi_\chi}{dT_B d\Omega} \right)_{3 \rightarrow 2} = \frac{\langle \sigma_{3 \rightarrow 2} v^2 \rangle}{24\pi m_A^3} \frac{dN}{dT_B} \int_{\text{l.o.s}} dl \rho_\chi^3(\mathbf{r}),$$

# DM boosted by astrophysical sources

## ☐ Sun (evaporation, reflection)

Kouvaris, et.al 1506.04316, An, et.al, 1708.03642

## ☐ Blazar/AGN (up-scattering)

Wang, et.al, arXiv:2202.07598,

## ☐ Supernova (up-scattering)

Lin, et.al, arXiv:2206.06864

## ☐ Supernova remnants (up-scattering)

Cappiello et.al, arXiv:2210.09448

## ☐ Blackholes (Hawking evaporation)

Calabrese, et.al, arXiv:2107.13001

Chao, et.al, arXiv:2108.05608

Kitabayashi, arXiv.2204.07898

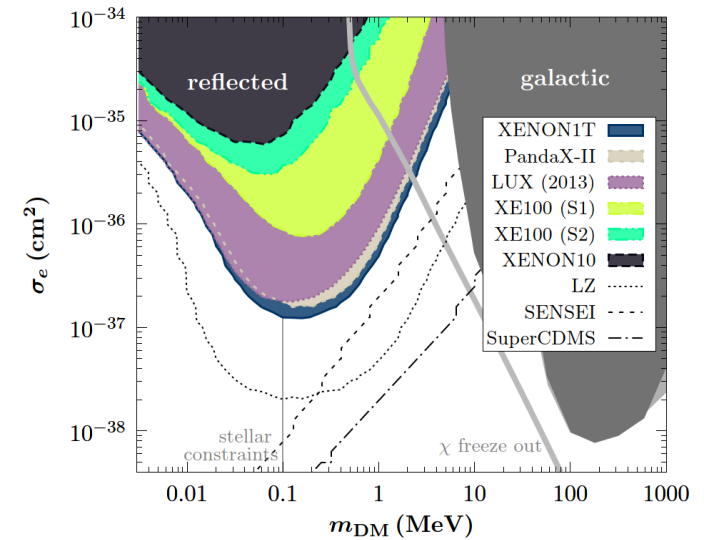
## ☐ Cosmic rays (up-scattering)

Bringmann, et.al, arXiv:1810.10543

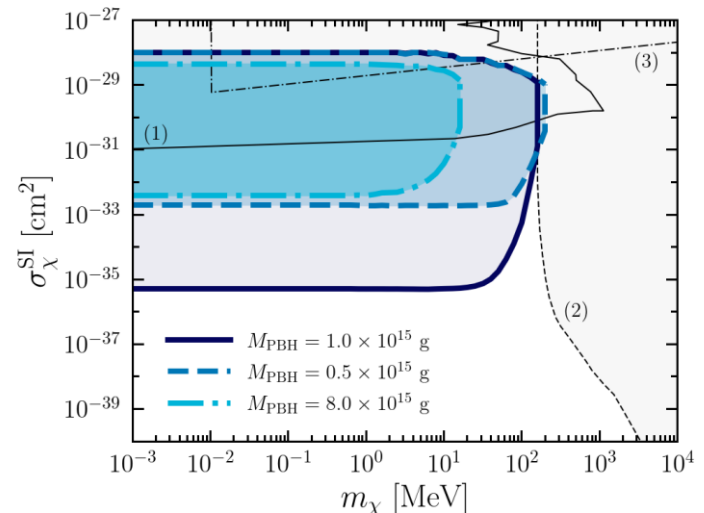
Ema, et.al, arXiv: 1811.00520

Cappiello, et.al, 1arXiv:906.11283

... ..



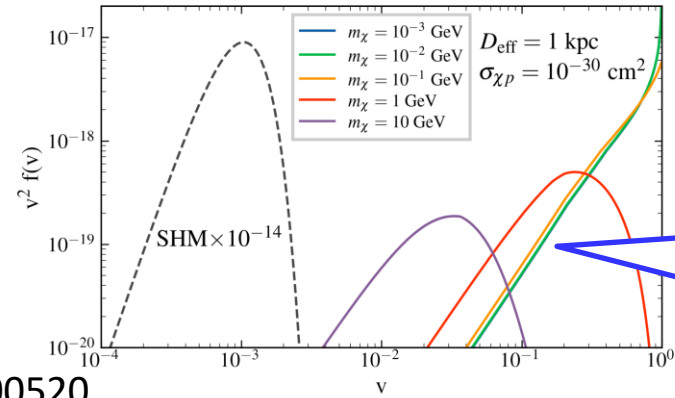
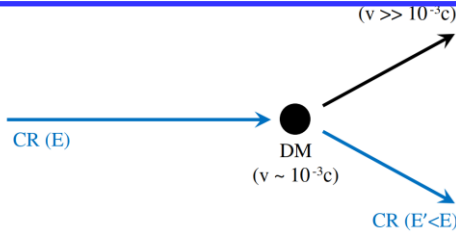
An, et.al, 1708.03642



Calabrese, et.al, arXiv:2107.13001

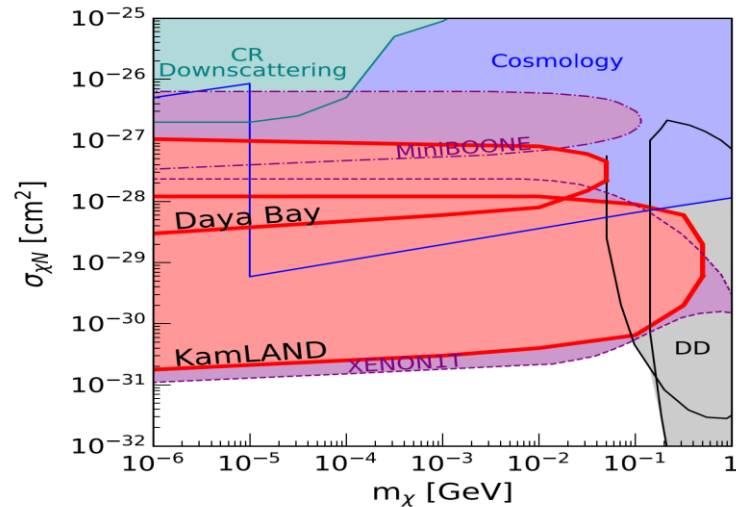
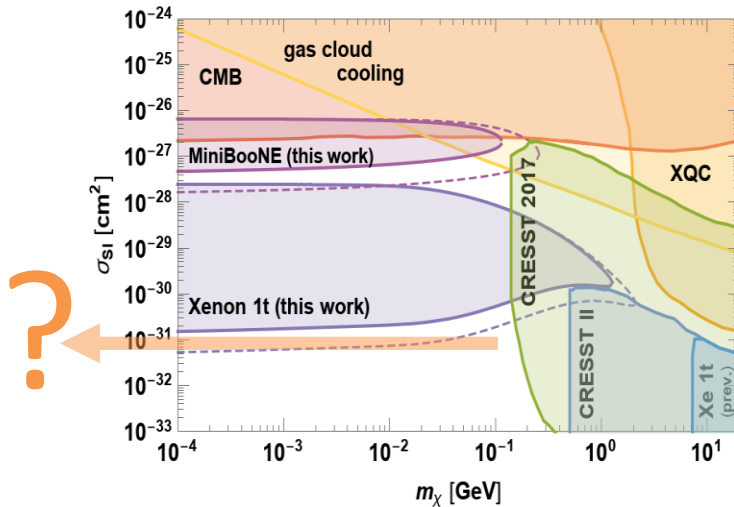
# CR-DM scattering: CR boosted dark matter

## CR boosted DM: Inverse direct detection



tiny DM component

Bringmann, et al 1810.10543, Y. Ema, et al, 1811.00520

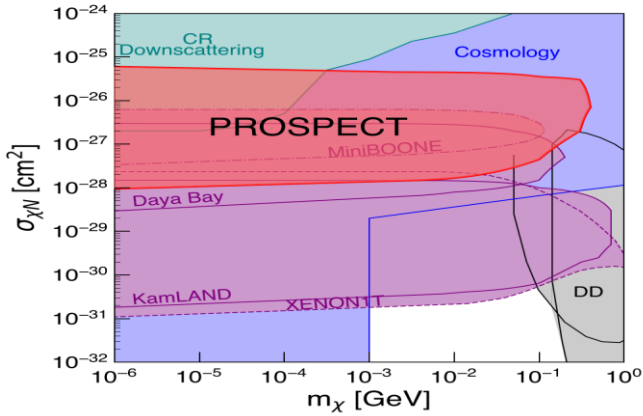


Cappiello, et al, (2019)

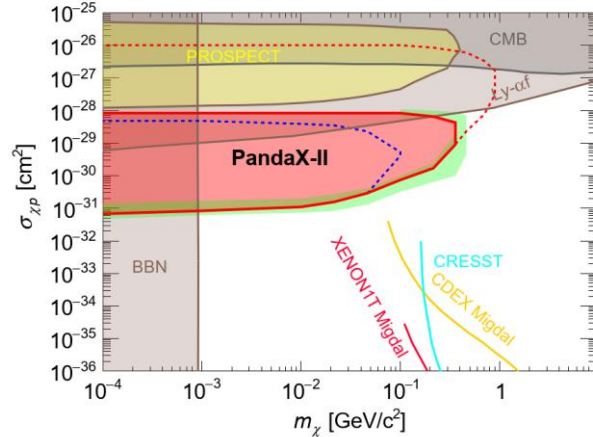
- ❑ Essentially no threshold problem
- ❑ Typical constraint  $\sigma_{\chi p} < 10^{-(31-32)} \text{ cm}^2$
- ❑ Constraints on  $\sigma_{\chi N}$  highly insensitive to DM mass

# Experimental searches for CRDM

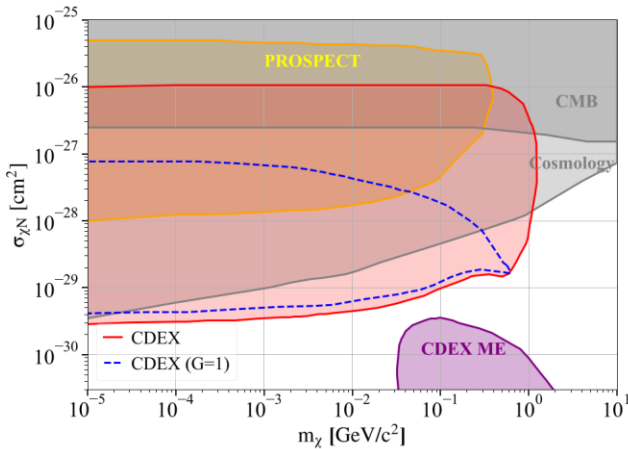
CR-boosted DM searched by virous experiments, e.g.



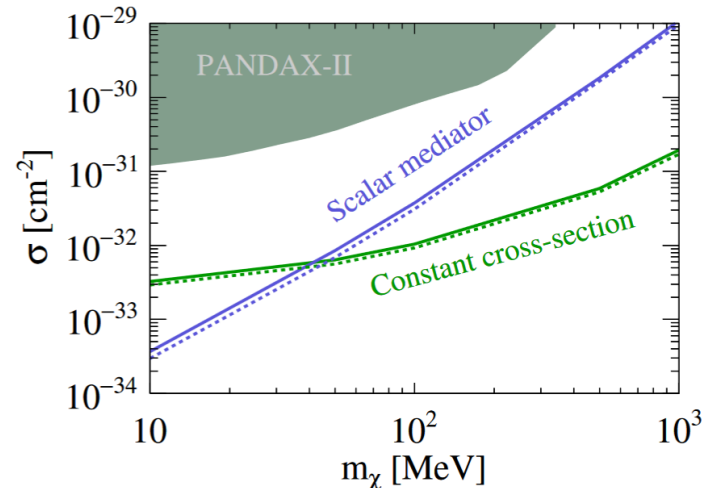
Prospect, arXiv:2104.11219



PandaX-II, arXiv:2112.08957



CDEX, arXiv:2201.01704



Super-K, arXiv:2209.14968

# The spectrum of CRDM

- DM flux from CR species  $i$ =proton, He, ...

$$\frac{d\Phi_\chi}{dT_\chi} = \int_{l.o.s} dl \int_{T_i^{\min}}^{\infty} dT_i \left( \frac{\rho_\chi}{m_\chi} \right) \left( \frac{d\sigma_{\chi i}}{dT_i} \right) \left( \frac{d\Phi_i}{dT_i} \right)$$

enhancement factor

drop rapidly towards higher E

- A simplification: CR flux is similar to the locally measured one  $\frac{d\Phi_i}{dT_i} \approx \frac{d\Phi_i^{LIS}}{dT_i}$

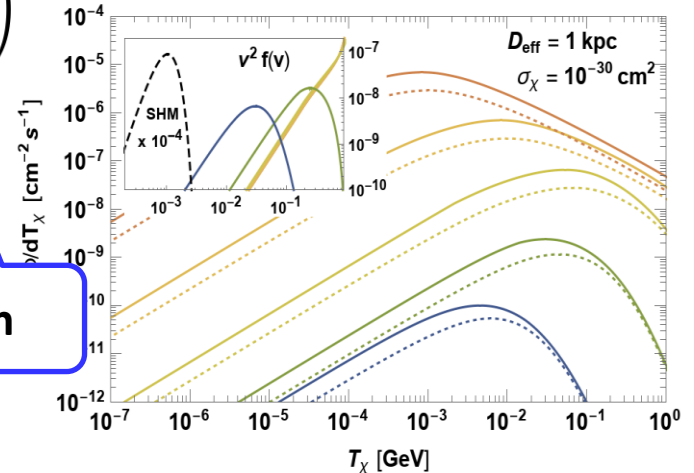
- The DM distribution can be factorized out (may not be accurate)

$$\frac{d\Phi_\chi}{dT_\chi} = \frac{\rho_\chi^{\text{loc}} D_{\text{eff}}}{m_\chi} \int_{T_i^{\min}}^{\infty} dT_i \left( \frac{d\sigma_{\chi i}}{dT_i} \right) \left( \frac{d\Phi_i^{\text{LIS}}}{dT_i} \right)$$

with

$$D_{\text{eff}} = \int_{l.o.s} dl \left( \frac{\rho_\chi}{\rho_\chi^{\text{loc}}} \right)$$

- Typical value of  $D_{\text{eff}} \sim$  a few kpc.



Bringmann, et al 1810.10543

# CRDM flux from a power-law CR source

a simple case: consider the CR flux (i=proton, He, etc. ) as a power-law (index  $\alpha$  ) with a cutoff (typical for diffusive shock wave acceleration by SNRs )

$$\frac{d\Phi_i^{\text{LIS}}}{d\gamma_i} = \Phi_i^0 \gamma_i^{-\alpha_i} \exp\left(-\frac{\gamma_i}{\gamma_{i,\text{cut}}}\right)$$

Analytical expression of the CRDM flux

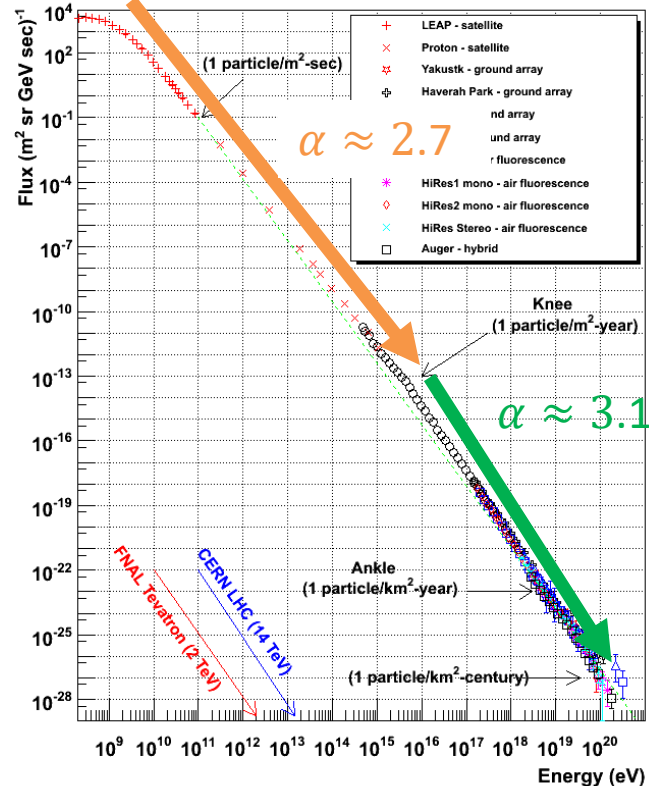
$$\frac{d\Phi_\chi}{dT_\chi} = \frac{\sigma_{\chi i} \rho_\chi^{\text{loc}} D_{\text{eff}} \Phi_i^0 F^2}{2m_\chi^2 \gamma_{i,\text{cut}}^{\alpha_i+1}} \Gamma(-(\alpha_i + 1), t)$$

asymptotic behavior

$$\Gamma(a, t) = \begin{cases} -t^a/a & (\text{for } t \ll 1) \\ t^{a-1} \exp(-t) & (\text{for large } t) \end{cases}$$

$$t = T_\chi / (2m_\chi \gamma_{i,\text{cut}}^2)$$

Cosmic Ray Spectra of Various Experiments



The observed CR all-particle spectrum



# For CR with $\sim E^{-3}$ , DM mass dependence disappears

1) before the cutoff, the CRDM is a power-law with a different power index

$$\frac{d\Phi_\chi}{dT_\chi} \approx \frac{2\sigma_{\chi i}\rho_\chi^{\text{loc}} D_{\text{eff}}\Phi_i^0 F^2}{\alpha_i + 1} T_\chi^{-2} \left(\frac{T_\chi}{2m_\chi}\right)^{(3-\alpha_i)/2}$$

□ DM spectrum: a power-law with index  $-(1 + \alpha)/2$

e.g.  $\frac{d\Phi}{dT} \approx T^{-2}$  for  $\alpha \approx 3$ ,

□ mass dependence:  $\sim m^{(\alpha-3)/2}$

DM flux becomes DM mass *independent*, provided  $\alpha = 3$

2) A final cutoff appears at  $T_{\chi,\text{cut}}^{\text{max}} = 2m_\chi \gamma_{i,\text{cut}}^2$

$$\frac{d\Phi_\chi}{dT_\chi} \approx \frac{\sigma_{\chi i}\rho_\chi^{\text{loc}} D_{\text{eff}}\Phi_i^0 F^2}{2m_\chi^2 \gamma_{i,\text{cut}}^{\alpha_i+1}} \left(\frac{T_\chi}{T_{\chi,\text{cut}}^{\text{max}}}\right)^{-\frac{\alpha_i+2}{2}} e^{-\left(\frac{T_\chi}{T_{\chi,\text{cut}}^{\text{max}}}\right)^{1/2}}$$

# Ultra-high energy CR: a power law $\sim E^{-3.1}$ up to $10^{20}$ eV

Indirect: **ground based** air-shower arrays

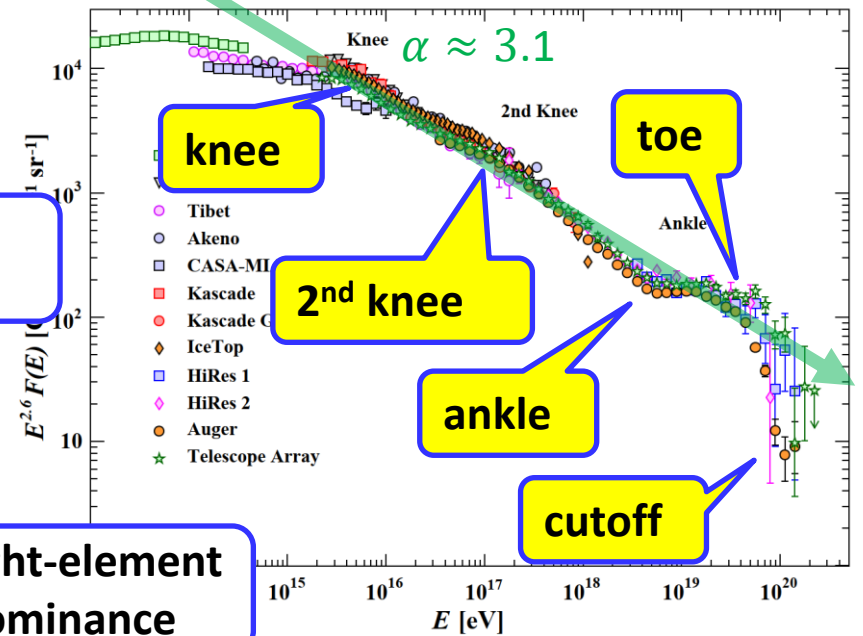
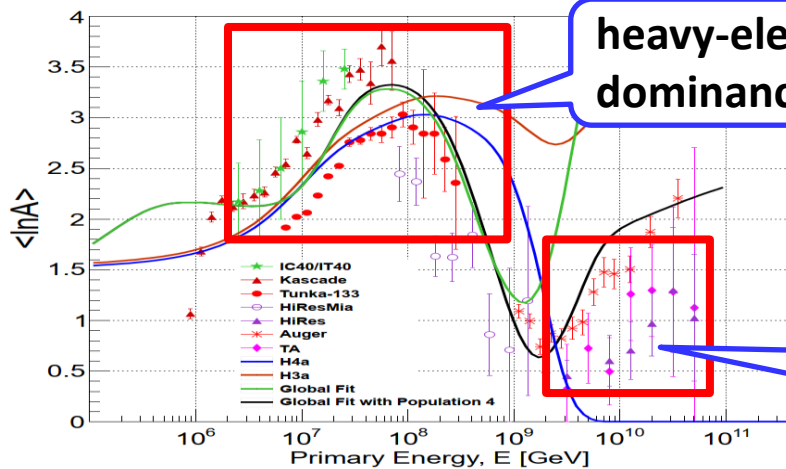
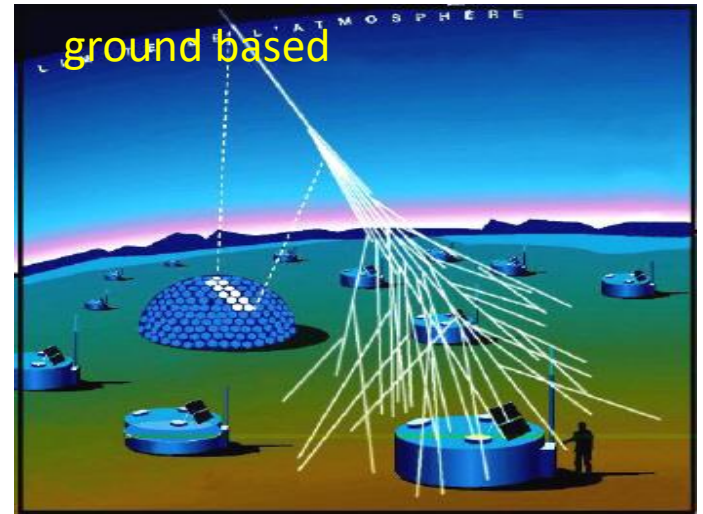
- ❑ Mass resolution limited to major groups
- ❑ Very large energy range:  $E \sim 10^{20}$  eV,

Spectral features in UHECR ( $E > \text{PeV}$ )

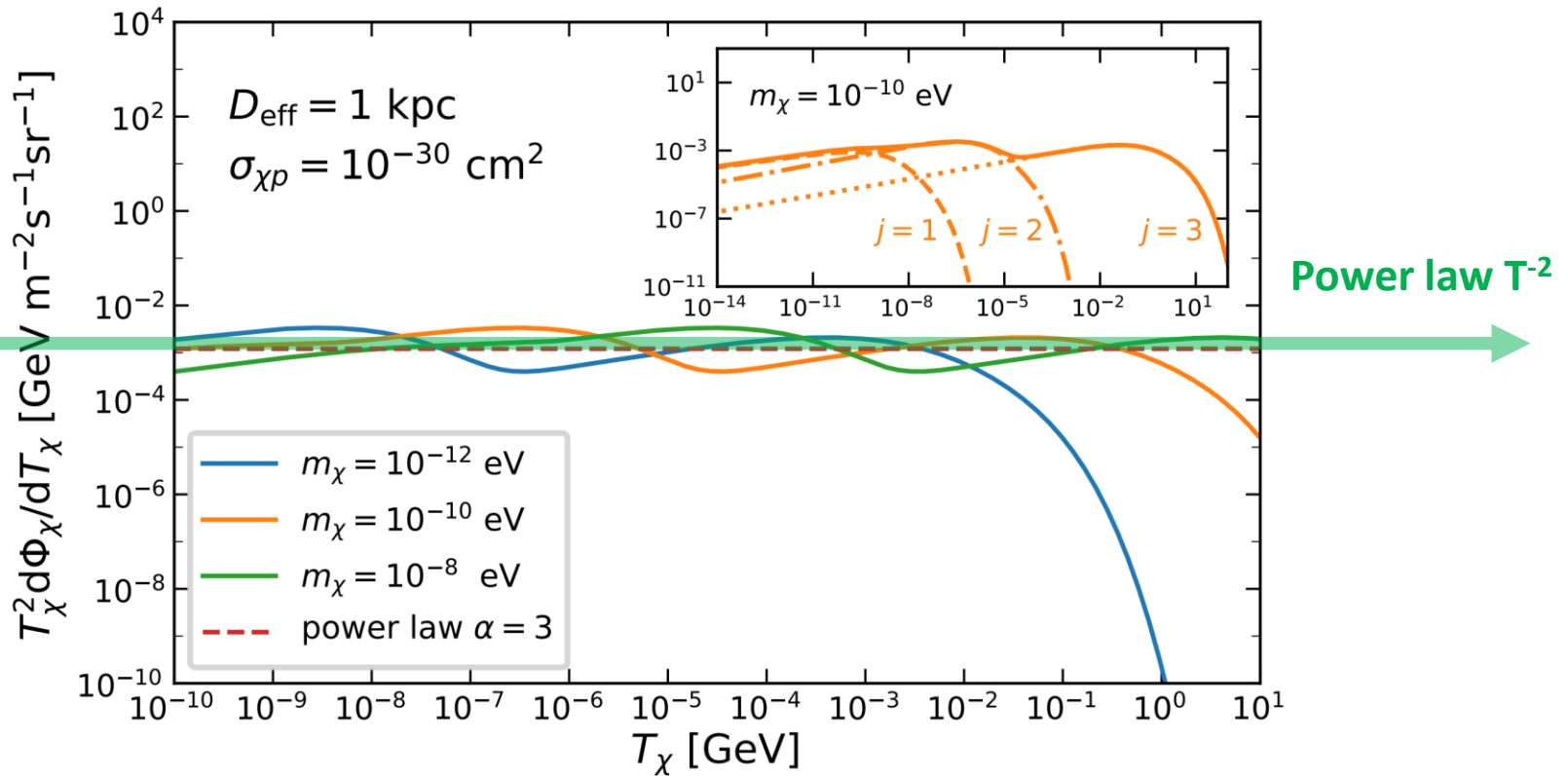
- 1) "knee" :  $3 \times 10^{15}$  eV
- 2) "second knee" :  $10^{17}$  eV
- 3) "ankle (dip)" :  $8 \times 10^{18}$  eV
- 4) "toe" :  $3 \times 10^{19}$  eV
- 5) "(GZK) cutoff"  $10^{20}$  eV

But, overall  $\alpha \approx 3$  is a good approximation

→ can speed up very low mass DM !



# CRDM powered by UHECR



- below the cutoff, CRDM flux for light DM is almost universal (direct consequence of  $\alpha \approx 3$ )
- Lighter DM reaches cutoff earlier

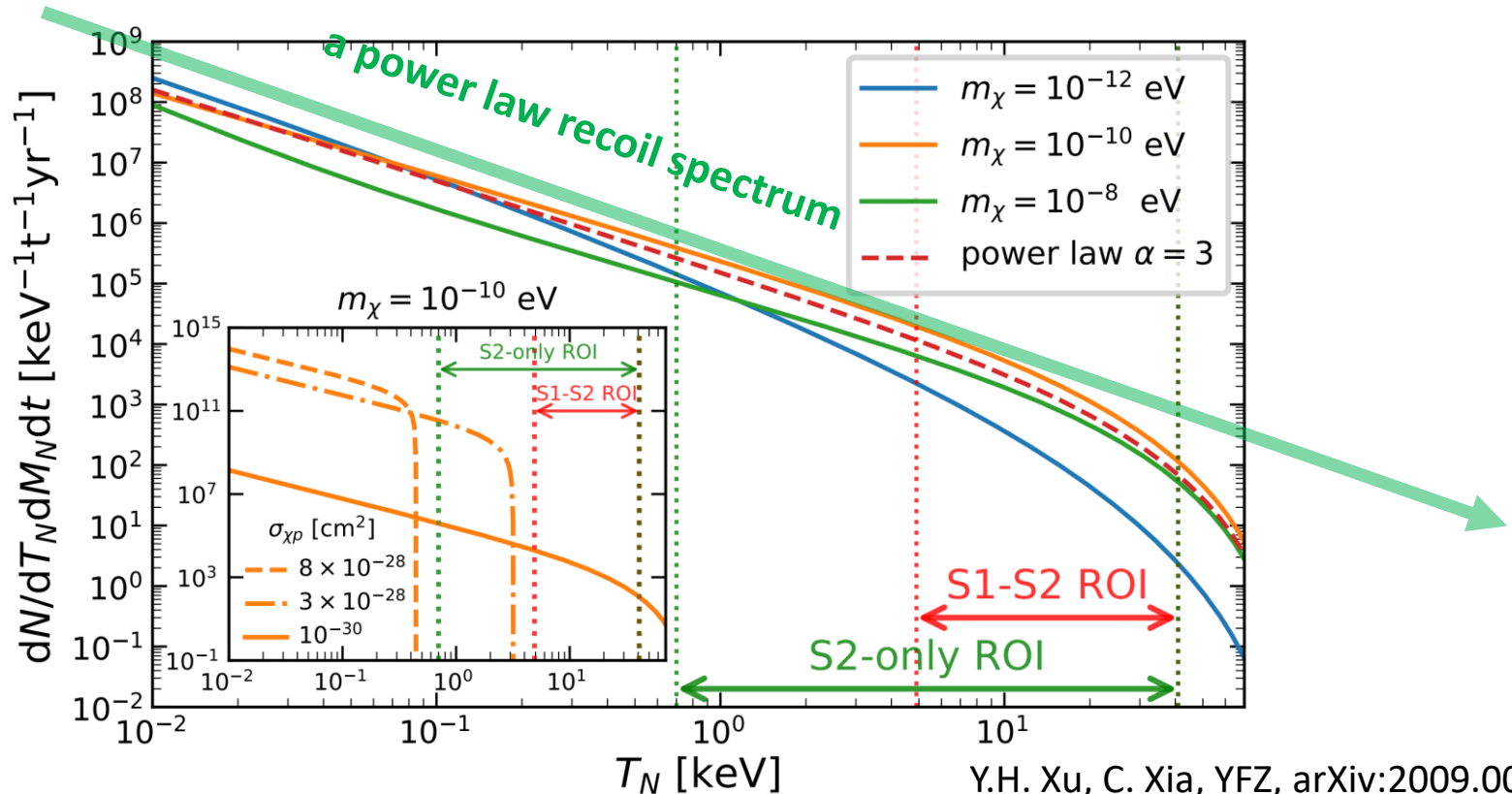
Y.H. Xu, C. Xia, YFZ, arXiv:2009.00353

# Nuclear recoil spectrum is also a power-law

(Neglecting the form factor)

Recoil event spectrum: a power law (not an exponential spectrum)

$$\Gamma \approx \frac{\pi \sigma_{\chi N} \sigma_{\chi i} \rho_{\chi} D_{\text{eff}} \Phi_i^0 F^2}{(1 + \alpha_i)(3 + \alpha_i) m_N^3} \left( \frac{m_N}{m_{\chi}} \right)^{\frac{3 - \alpha_i}{2}} \left( \frac{T_N}{8m_N} \right)^{-\frac{3 + \alpha_i}{4}}$$



Y.H. Xu, C. Xia, YFZ, arXiv:2009.00353

# Constraining CRDM in LXe detectors

natively rescaling the known WIMP search limits is NOT accurate

- Total number of quantum for given  $T_N$

$$N_q = N_{ex} + N_i = \text{Bino}(T_N/W, L)$$

work function  $W = 13.8 \text{ eV}$ .

- The Linderhard factor

$$L = \frac{kg(\epsilon)}{1 + kg(\epsilon)}$$

- Number of ions

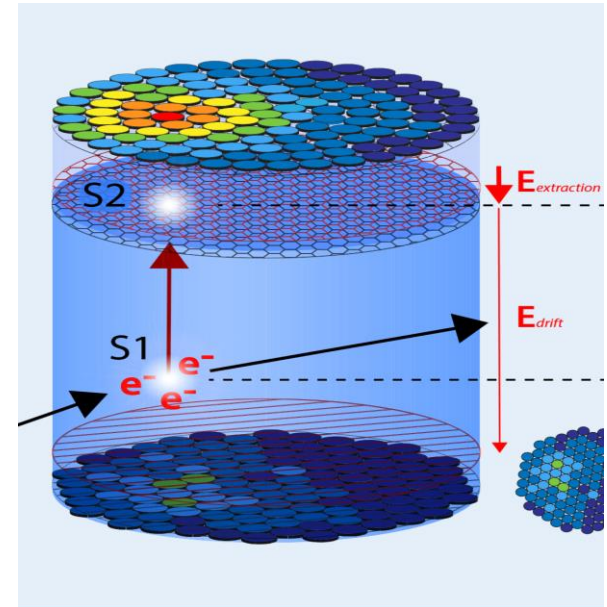
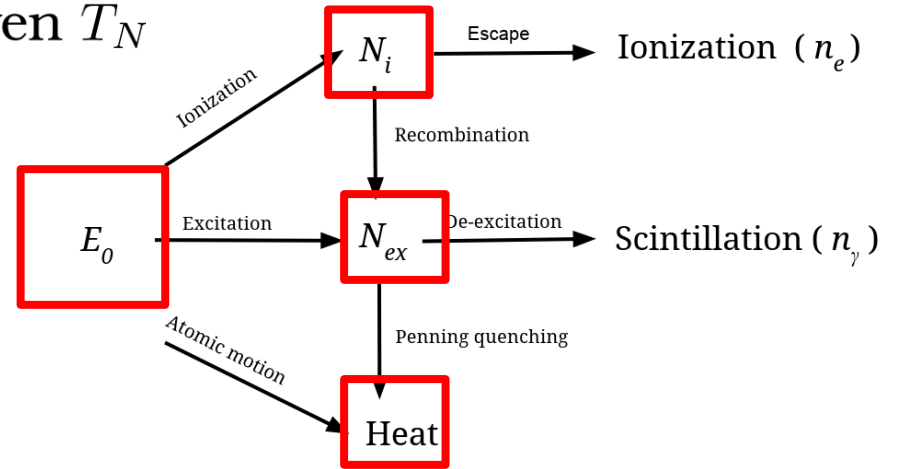
$$N_i = \text{Bino}(N_q, 1/(1 + \langle N_{ex}/N_i \rangle))$$

$$N_{ex} = N_q - N_i$$

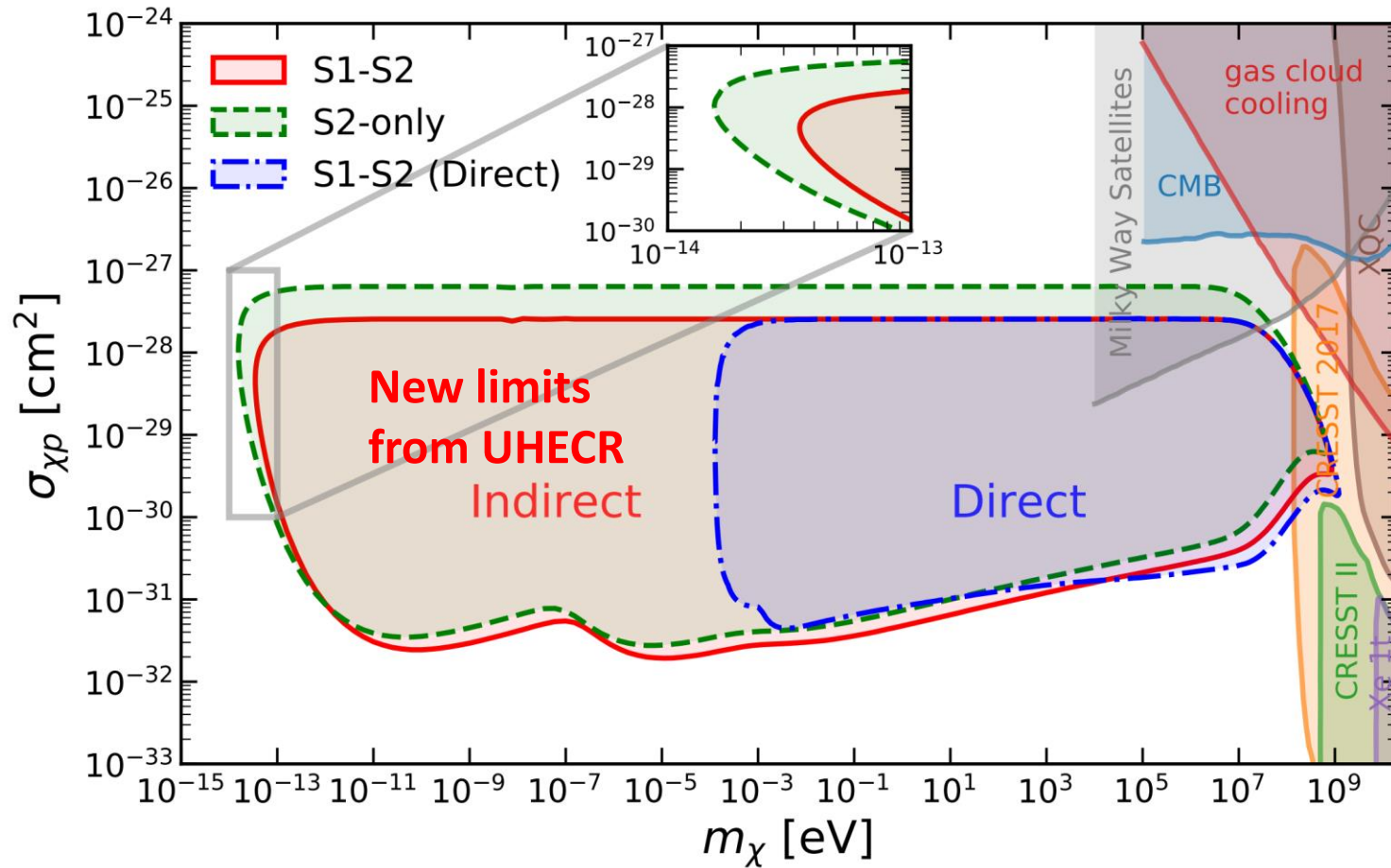
- Number of electrons and photons

$$N_e = \text{Bino}(N_i, 1 - r)$$

$$N_\gamma = N_{ex} + N_i - N_e$$



# Constraints from Xenon-1T



Using UHECR, the limits can be extended down to ultra-low mass region

Y.H. Xu, C. Xia, YFZ, arXiv:2009.00353

# BBN constraints (model dependent)

Any thermalized light species below MeV scale is constrained by BBN

Typical thermalization condition  $\sigma_{\chi q} \leq 10^{-46} \text{cm}^2$ . G.Krnjaic et.al, 1908.00007

## Typical mass limits for benchmark models:

- ❑ Hardphilic DM: 0.9 MeV (real scalar), 5.3 MeV (complex scalar), 5.0 MeV (Majorana fermion)  
7.8 GeV (Dirac fermion), G.Krnjaic et.al, 1908.00007
- ❑ Electrophilic DM: 0.4 MeV (real scalar), 0.5 MeV (complex scalar),  
0.5 MeV (Majorana fermion) 0.7 GeV (Dirac fermion), Sabti, et. al, 1910.01649

## Assumptions implied in BBN constraints

- ❑ DM mass is time-independent
- ❑ DM-nucleon coupling is time-independent
- ❑ Scattering/annihilation are of the same order of magnitude (typically 2-2)
- ❑ Standard cosmology (Hubble tension issue)

## Exceptions:

- ❑ DM may become lighter today (change in VEV),  
e.g. the *morphon* models, Croon et.al, arXiv:2012.15284
- ❑ DM interactions depends on the local DM density ,  
e.g. the *chameleon* models, K. Boddy et.al, arXiv:1208.4376
- ❑ DM interactions stronger today due to PhT (reduced mediator mass)  
e.g. *HYPER* DM, G. Elor et.al, arXiv:2112.03920

**CRDM limits are based on the measurement of the present-day, local Universe, which is complementary to those from BBN and CMB**

# The ceiling: Earth attenuation (for constant $\sigma_{\chi N}$ )

simple mean-free-path based estimation

relativistic

$$\frac{dT_\chi}{dz} = - \left( \frac{T_\chi}{\ell_E} + \frac{T_\chi^2}{2m_\chi \ell_E} \right)$$

mean-free-path for  $E$ -loss

non-relativistic

$$\ell_E \approx 3 \text{ km} \left( \frac{10^{-27} \text{ cm}^2}{\sigma_{\chi p}} \right) \left( \frac{\text{MeV}}{m_\chi} \right)$$

• relativistic limit

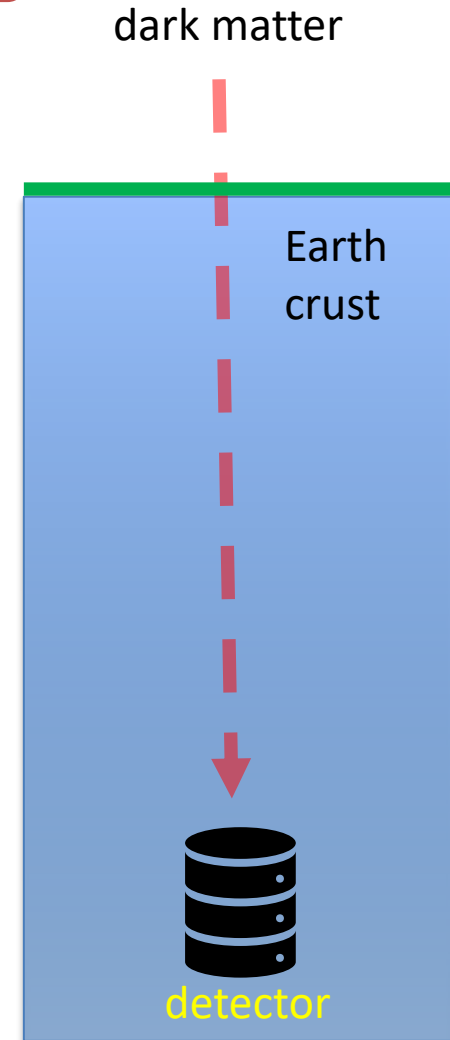
$$T_\chi(z) = \frac{T_\chi(0)}{1 + \frac{T_\chi(0)z}{2m_\chi \ell_E}}$$

Non-relativistic limit  $T_\chi(z) = T_\chi(0)e^{-z/\ell_E}$

Energy-independent cutoff for  $T_\chi(0) \rightarrow \infty$

$$T_\chi^{\text{max}}(z) \rightarrow \frac{2m_\chi \ell_E}{z}$$

If  $T_\chi^{\text{max}}(z)$  is too small, DM cannot be detected





# Energy cutoff due to Earth attenuation

Consider spin-independent, isospin conserving case  $\sigma_{\chi T} \approx A^2 \sigma_{\chi p}$   
 mass of the nucleus  $m_T \approx Am_p$

Consequence:

1) the mean-free-path

$$\ell_E^{-1} \approx \frac{2\rho_{\oplus}\sigma_{\chi p}m_{\chi}}{m_p^2}$$

independent of the chemical composition of the crust

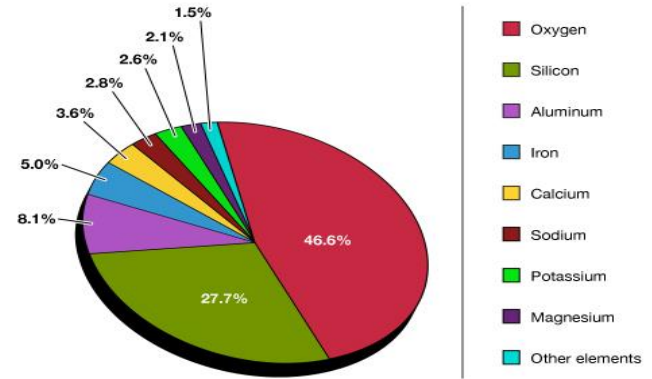
2) the cutoff energy

$$T_{\chi}(z) \rightarrow \frac{m_p^2}{z\rho_{\oplus}\sigma_{\chi p}}$$

DM mass  $m_{\chi}$  independent

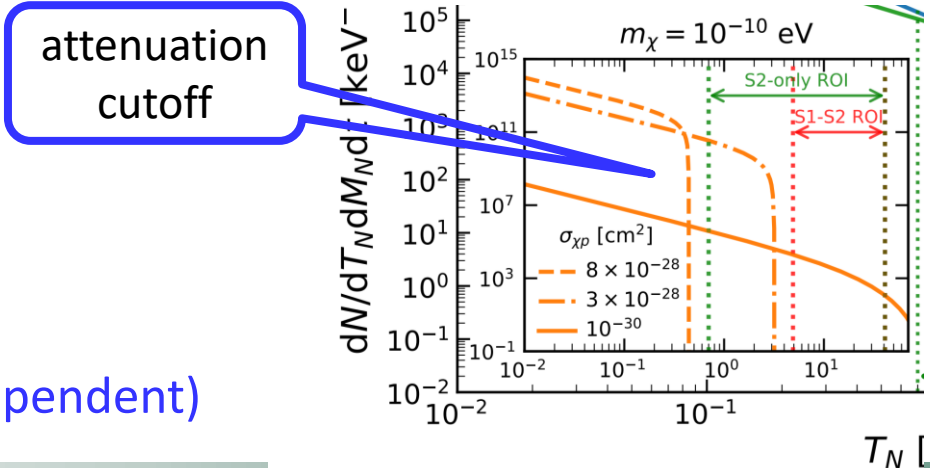
Detection blind spot is DM mass independent)

Composition of Earth's Crust



Source: United States Geological Survey

© Encyclopædia Britannica, Inc.



# nuclear form factor effect (energy-dependent cross section)

Even in the simplest case,

Form factor introduce additional E-dependence to  $\sigma_{\chi N}$

$$R(T_\chi) \equiv \frac{\sigma_{\chi N}}{\sigma_{\chi N}^0} = \int_0^{T_N^{\max}(T_\chi)} \frac{F^2(q^2)}{T_N^{\max}(T_\chi)} dT_N,$$

The Helm form factor

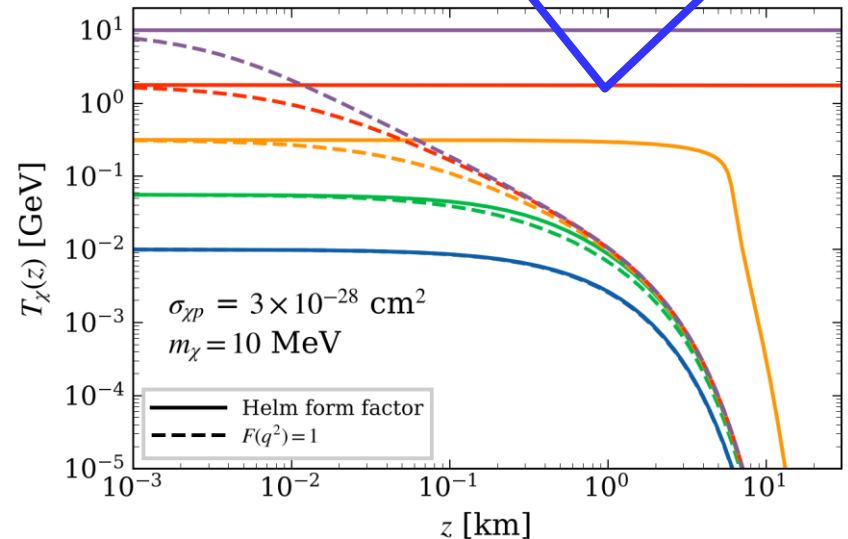
$$F(q^2) = \frac{3j_1(qR_1)}{qR_1} e^{-\frac{1}{2}q^2 s^2}$$

can be approximated as  $F(q^2) \approx e^{-q^2/\Lambda^2}$

$$\frac{dT_\chi}{dz} \approx -\frac{1}{2} \sum_N n_N \sigma_{\chi N}^0 T_N^{\max} f(4m_N T_N^{\max} / \Lambda_N^2),$$

the energy suppression of  $T_\chi(z)$  is reduced

attenuation negligible for high-energy DM due to the form factor effect

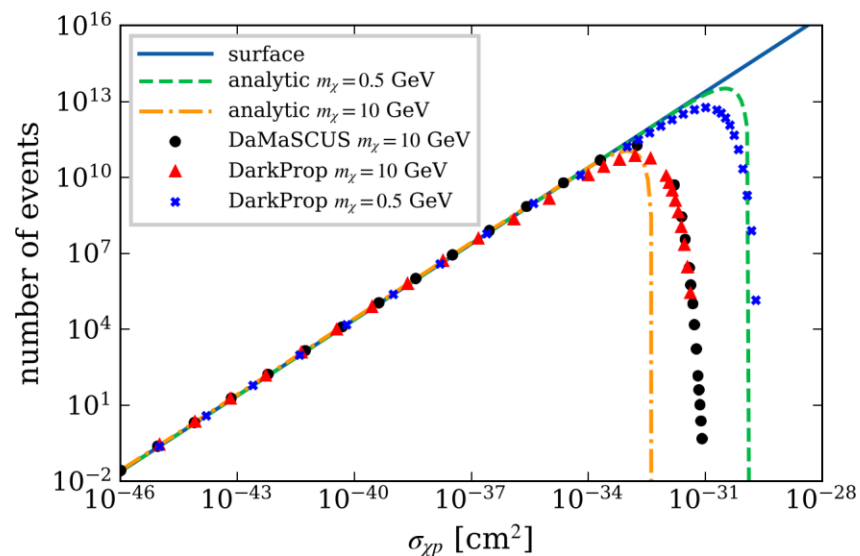
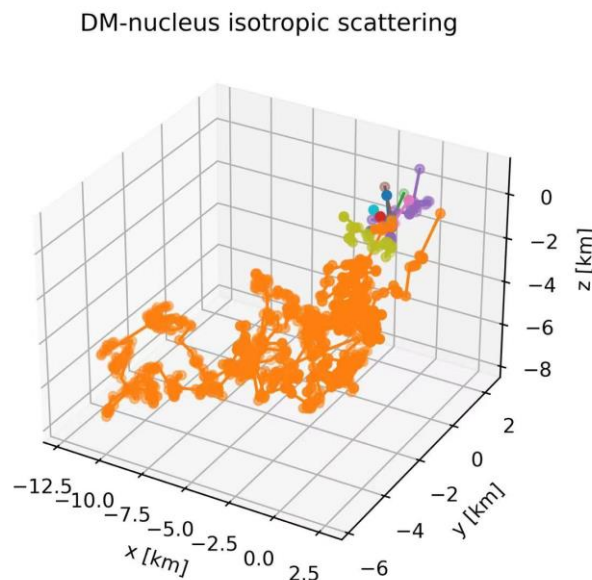


$$T_\chi^3(z) \approx T_\chi^3(0) - \frac{3z}{32} \sum_N n_N \sigma_{\chi N}^0 \frac{\Lambda_N^4}{m_N}.$$

Y.H. Xu, C. Xia, YFZ, arXiv:2011.05559

# DarkProp: a code for simulation DM propagation in the Earth

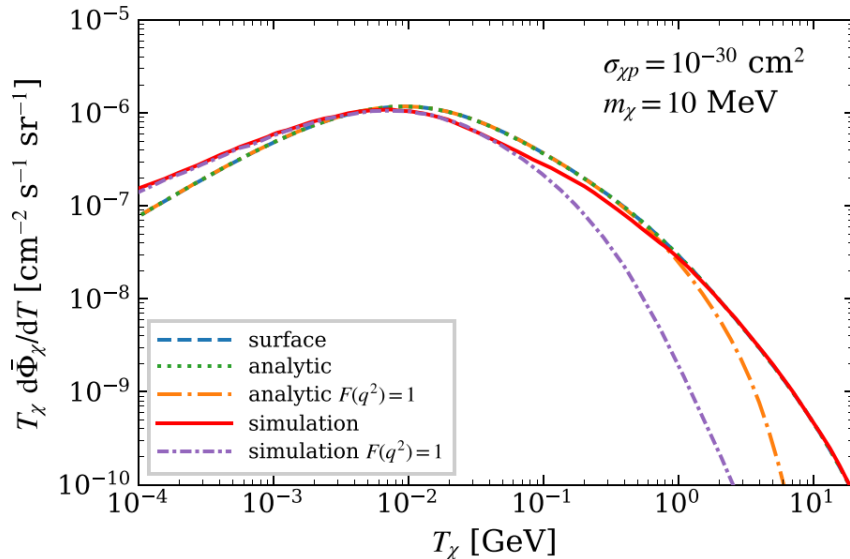
- Isotropic initial condition (to be updated to anisotropic case)
- A simple Earth model with chemical composition included
- For both relativistic and non-relativistic scattering
- Nuclear form factor implemented
- Cross-checked with DaMaSCUS



<http://yfzhou.itp.ac.cn/darkprop>

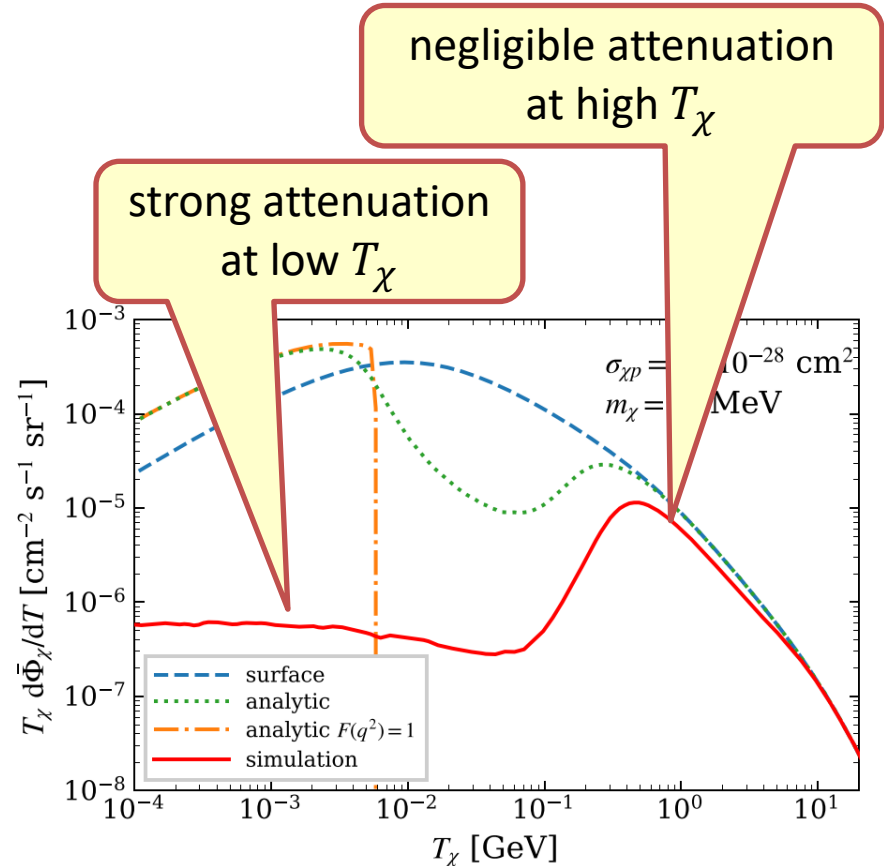
# Underground DM flux from simulations

Underground DM spectrum is significantly distorted for large  $\sigma_{\chi p}$



small cross section case

$$\sigma_{\chi p} = 10^{-30} \text{ cm}^2$$



large cross section case

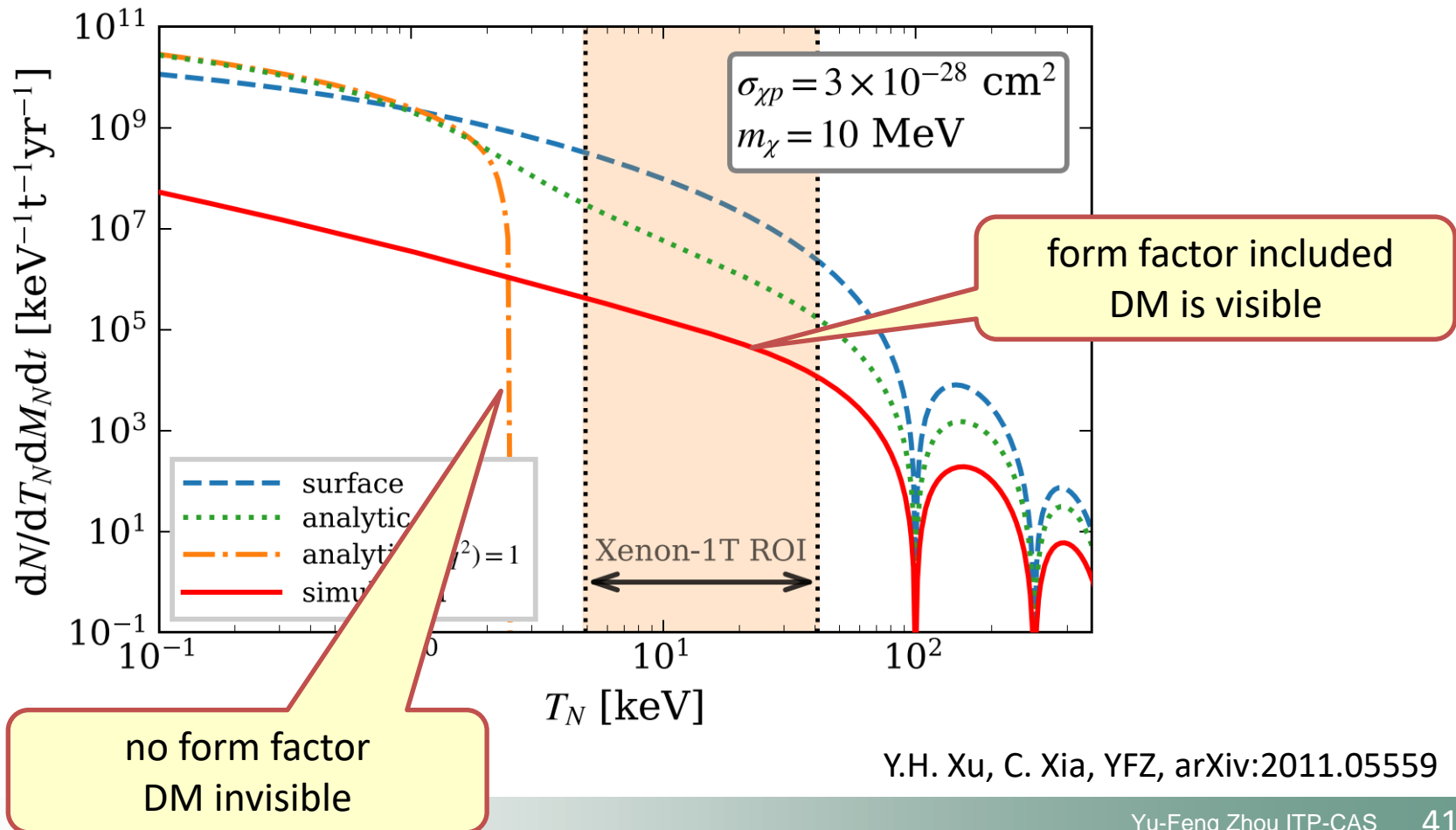
$$\sigma_{\chi p} = 10^{-28} \text{ cm}^2$$

Y.H. Xu, C. Xia, YFZ, arXiv:2011.05559

# Large cross section now can be probed

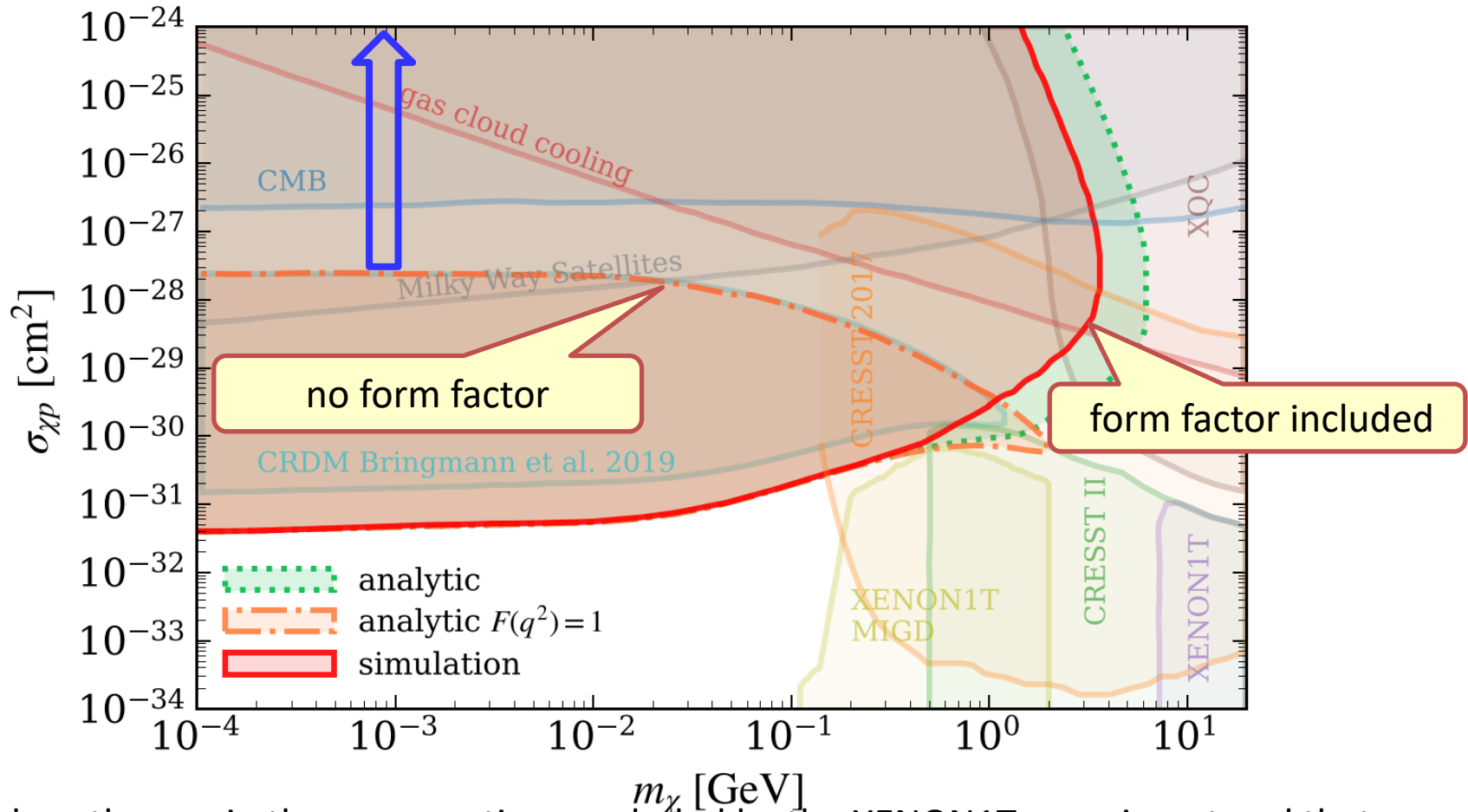
No spectrum cut off any more

DM particles can enter Xenon-1T ROI with large event rates



# (almost) no ceiling for CRDM

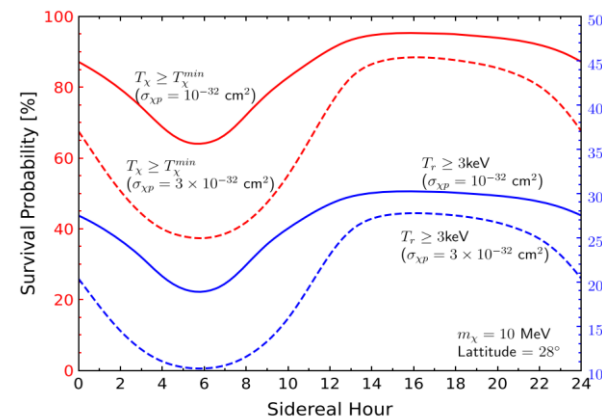
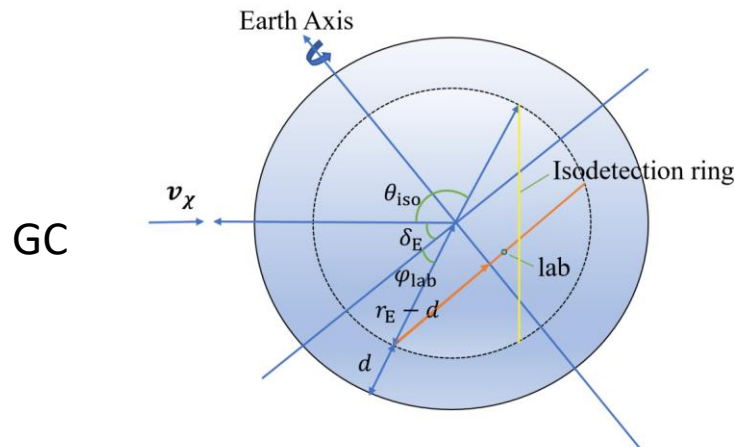
Y.H. Xu, C. Xia, YFZ, arXiv:2011.05559



close the gap in the cross sections excluded by the XENON1T experiment and that by the astrophysical measurements such that for the cosmic microwave background (CMB), galactic gas cloud cooling, and structure formation, etc..

# Angular distribution of CRDM

- ❑ CRDM has a preferred direction due to
  - inhomogeneous distribution of DM profile (centered towards GC)
  - inhomogeneous distribution of CRs (not centered towards GC)
  
- ❑ Most of the current DM detection exps. cannot distinguish direction
  - Observables: scintillation, ionization, heat
  
- ❑ For large enough  $\sigma_{\chi p}$ , if the earth attenuation is significant, diurnal modulation of the event rate may appear due to the anisotropic CRDM flux



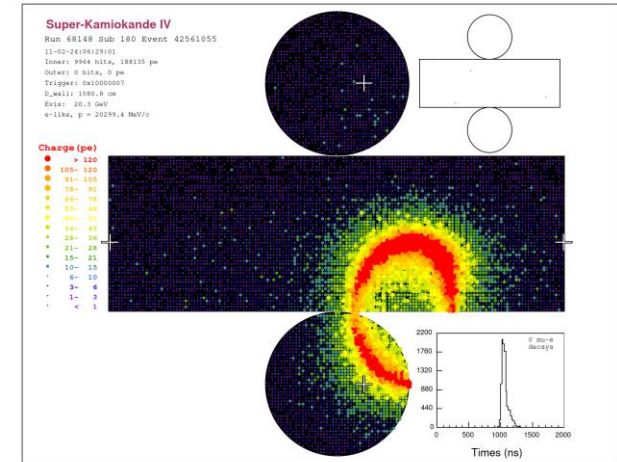
Ge, et al, arXiv2005.09480

# Probing the morphology of CRDM flux

## Cherenkov detectors can tell the arrival direction of DM

### Detectors for neutrino experiments

- 1) **Liquid scintillator** detectors: *Borexino, DUNE*  
Low threshold (keV), no direction identification
- 2) **Water Cherenkov** detectors: *Super-K, SNO*  
High threshold (MeV), can measure direction
- 3) **Hybrid** detectors, 1)+2): SNO+



For boosted DM, the threshold is no longer a problem --> good news for neutrino experiments

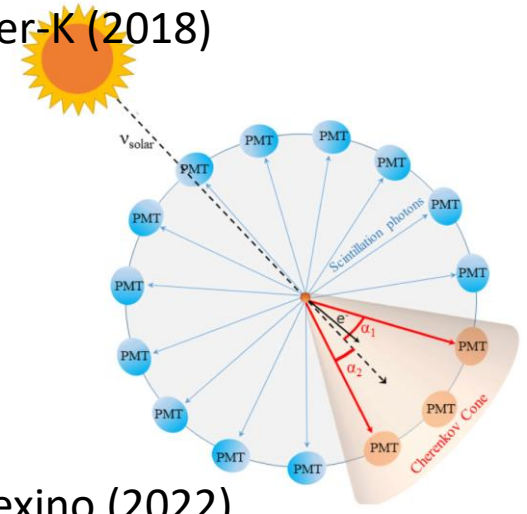
☐ neutrino Exps. have huge exposures

e.g. SK: 50 kt

☐ Water Cherenkov detectors can measure direction  
recoil electrons (and protons) following the direction of DM

SK has good angular resolution  $\sim 3^\circ$

elastic electron scattering  
Super-K (2018)



Borexino (2022)



# Unique morphological feature of the CRDM flux

Distribution of DM flux close follows the sources

- DM boosted by the Sun, supervona, etc, **point-like**
- DM boosted by the dark sector **diffuse, azimuthal symmetric**

- decay 
$$\left(\frac{d\Phi_\chi}{dT_B d\Omega}\right)_{\text{dec}} = \frac{1}{4\pi m_A \tau_A} \frac{dN}{dT_B} \int_{\text{l.o.s}} dl \rho_\chi(\mathbf{r}),$$

- annihilation 
$$\left(\frac{d\Phi_\chi}{dT_B d\Omega}\right)_{\text{ann}} = \frac{\langle \sigma_{\text{ann}} v \rangle}{8\pi m_A^2} \frac{dN}{dT_B} \int_{\text{l.o.s}} dl \rho_\chi^2(\mathbf{r}),$$

- 3 → 2 process 
$$\left(\frac{d\Phi_\chi}{dT_B d\Omega}\right)_{3 \rightarrow 2} = \frac{\langle \sigma_{3 \rightarrow 2} v^2 \rangle}{24\pi m_A^3} \frac{dN}{dT_B} \int_{\text{l.o.s}} dl \rho_\chi^3(\mathbf{r}),$$

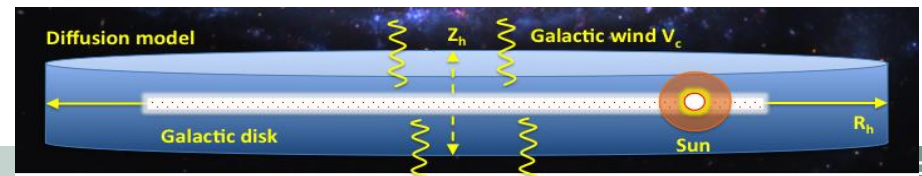
- DM boosted by CRs **diffuse, azimuthal asymmetric**

$$\frac{d\Phi_\chi}{dT_\chi d\Omega} = \int_{\text{l.o.s}} dl \frac{\rho_\chi(\mathbf{r})}{m_\chi} \int_{T_e^{\min}} dT_e \frac{\sigma_{\chi e}}{T_\chi^{\max}} \frac{d\Phi_e(\mathbf{r})}{dT_e},$$

Distribution of CR source

$$q(R, z) = \left(\frac{R}{R_\odot}\right)^a \exp\left(-b \frac{R - R_\odot}{R_\odot}\right) \exp\left(-\frac{|z|}{z_s}\right),$$

Diffusion halo  $z_h \ll R_h$



# Azimuthal symmetry breaking in CRDM flux

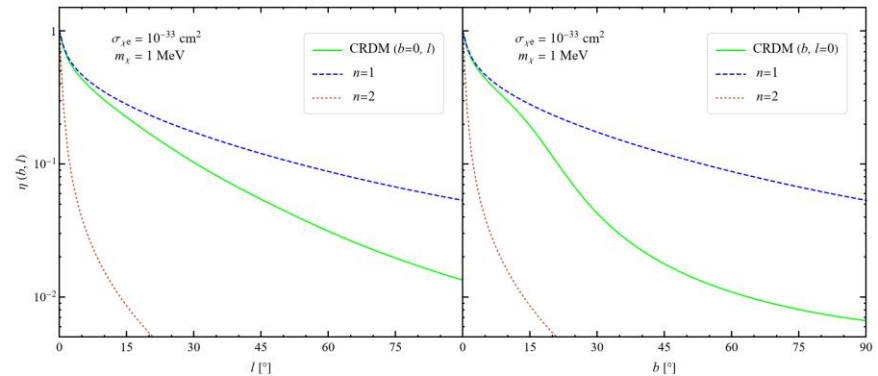
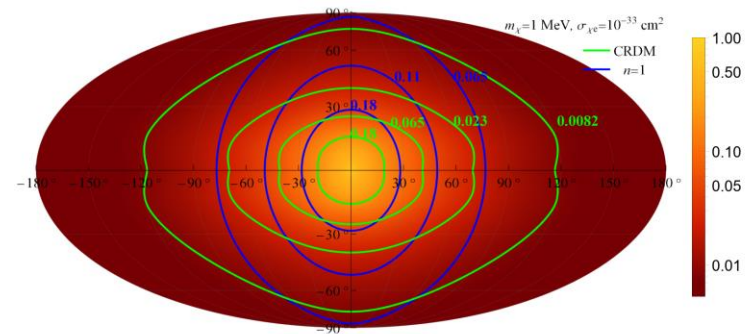
Harmonic expansion

$$\frac{d\Phi_\chi}{d\Omega}(\theta, \varphi) = \sum_{l=0}^{\infty} \sum_{m=-l}^l a_{l,m} Y_{l,m}(\theta, \varphi),$$

Coefficients

$$a_{l,m} = \int d\Omega Y_{l,m}^*(\theta, \varphi) \frac{d\Phi_\chi}{d\Omega}(\theta, \varphi).$$

- $a_{l,m}$  independent of  $\sigma_{\chi e}$
- nonvanishing  $a_{l,m}$  with  $m \neq 0$   
 $\rightarrow$  azimuthal symmetry breaking

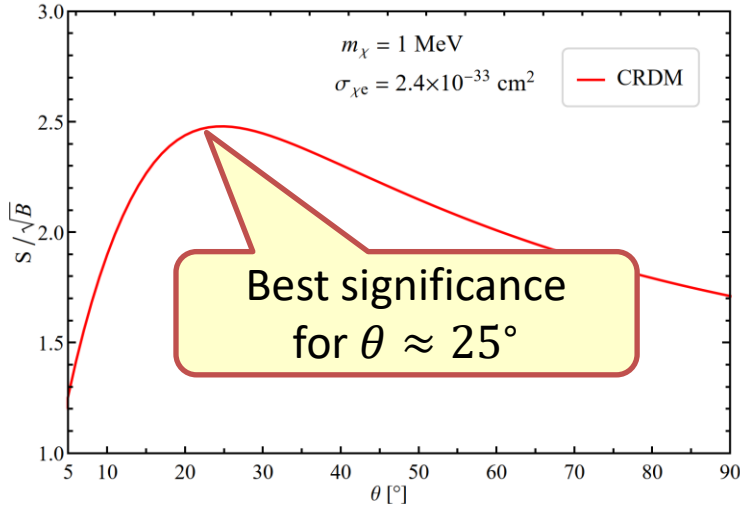


		$\tilde{a}_{1,0}$	$\tilde{a}_{2,0}$	$\tilde{a}_{3,0}$	$\tilde{a}_{4,0}$	$\tilde{a}_{5,0}$	$\tilde{a}_{2,2}$	$\tilde{a}_{3,2}$	$\tilde{a}_{4,2}$	$\tilde{a}_{4,4}$	$\tilde{a}_{5,2}$	$\tilde{a}_{5,4}$
NFW	CRDM	1.00	0.90	0.77	0.63	0.52	0.12	0.12	0.11	0.02	0.09	0.02
	BDM ( $n=1$ )	0.63	0.37	0.24	0.17	0.13	0	0	0	0	0	0
	BDM ( $n=2$ )	1.28	1.33	1.32	1.29	1.27	0	0	0	0	0	0
Einasto	CRDM	1.06	1.00	0.88	0.75	0.64	0.11	0.11	0.10	0.02	0.09	0.02
	BDM ( $n=1$ )	0.68	0.43	0.30	0.22	0.17	0	0	0	0	0	0
	BDM ( $n=2$ )	1.36	1.46	1.47	1.45	1.42	0	0	0	0	0	0

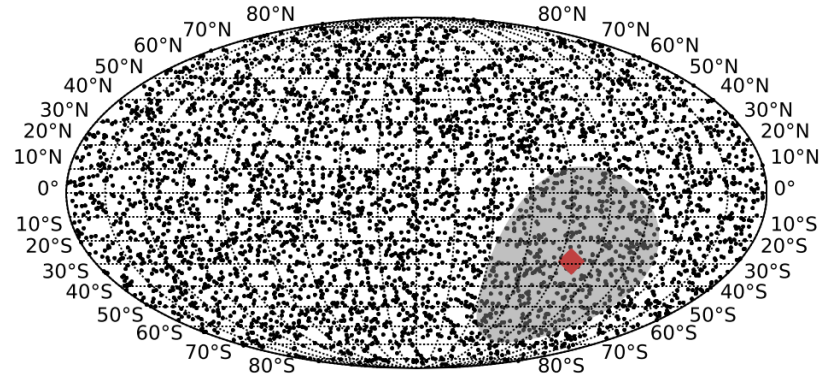
symmetry breaking term

# Constraints on DM-electron scattering from SK-IV data

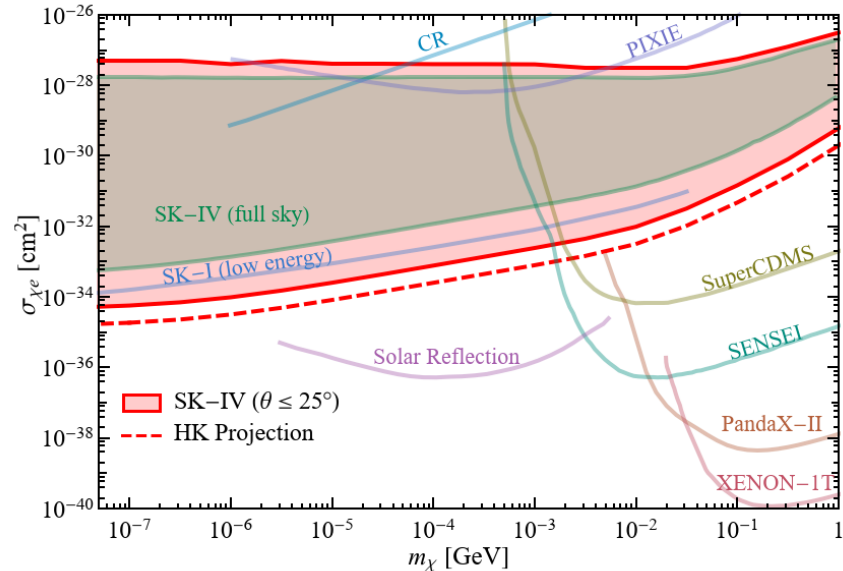
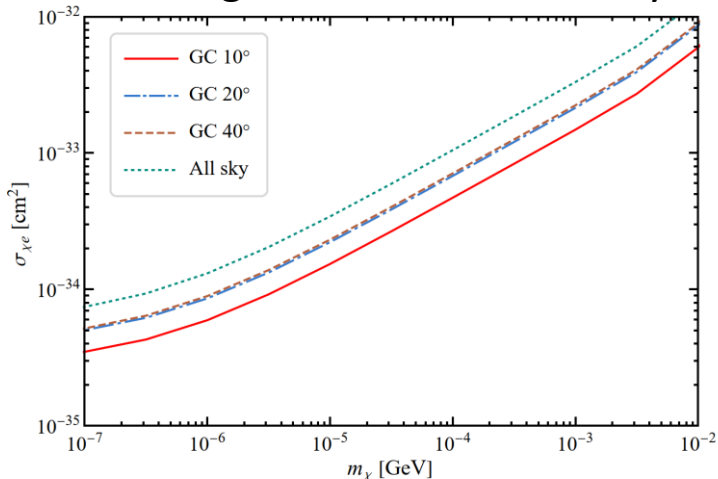
Optimize the search cone



SK-IV all-sky data, 0.1–1.33 GeV



SK-IV background level: 1.96/kt/yr/sr



So far the most stringent limit

$$\sigma_{\chi e} \leq 2.4 \times 10^{-33} \text{ cm}^2 @ 1 \text{ MeV}$$

Limits at different cut-angles  $\theta$

# Distinguishing CRDM from other boosted DM models

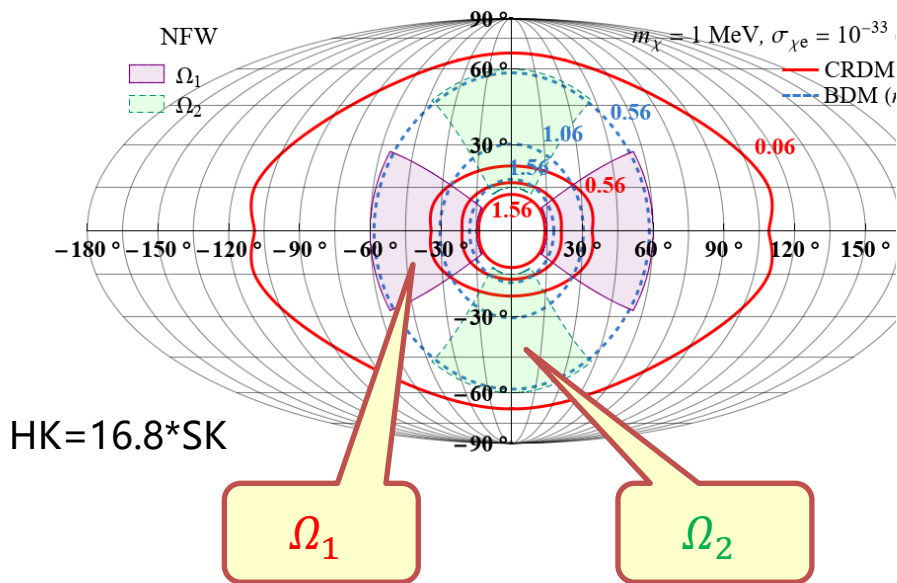
Define an azimuthal asymmetric parameter

$$A_R = \frac{N(\Omega_1) - N(\Omega_2)}{N(\Omega_1) + N(\Omega_2)},$$

Regions  $\Omega_1$  and  $\Omega_2$  are related by a  $90^\circ$  rotation

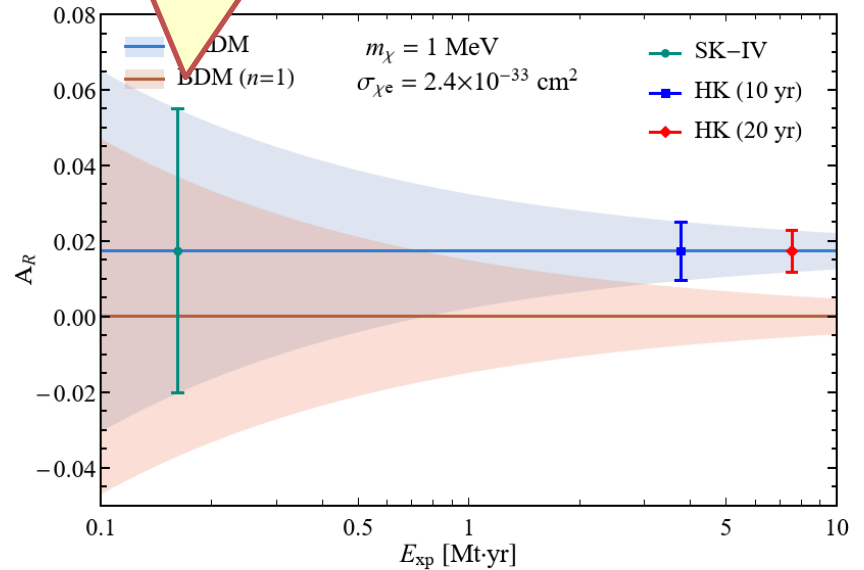
Optimize  $\Omega_1/\Omega_2$  to maximize  $A_R$

According to the SK background rate



future  $A_R^{HK} = 0.017 \pm 0.0055$

now  $A_R^{SK} = 0.017 \pm 0.036$



CRDM can be distinguished from other boosted DM models

# Summary

---

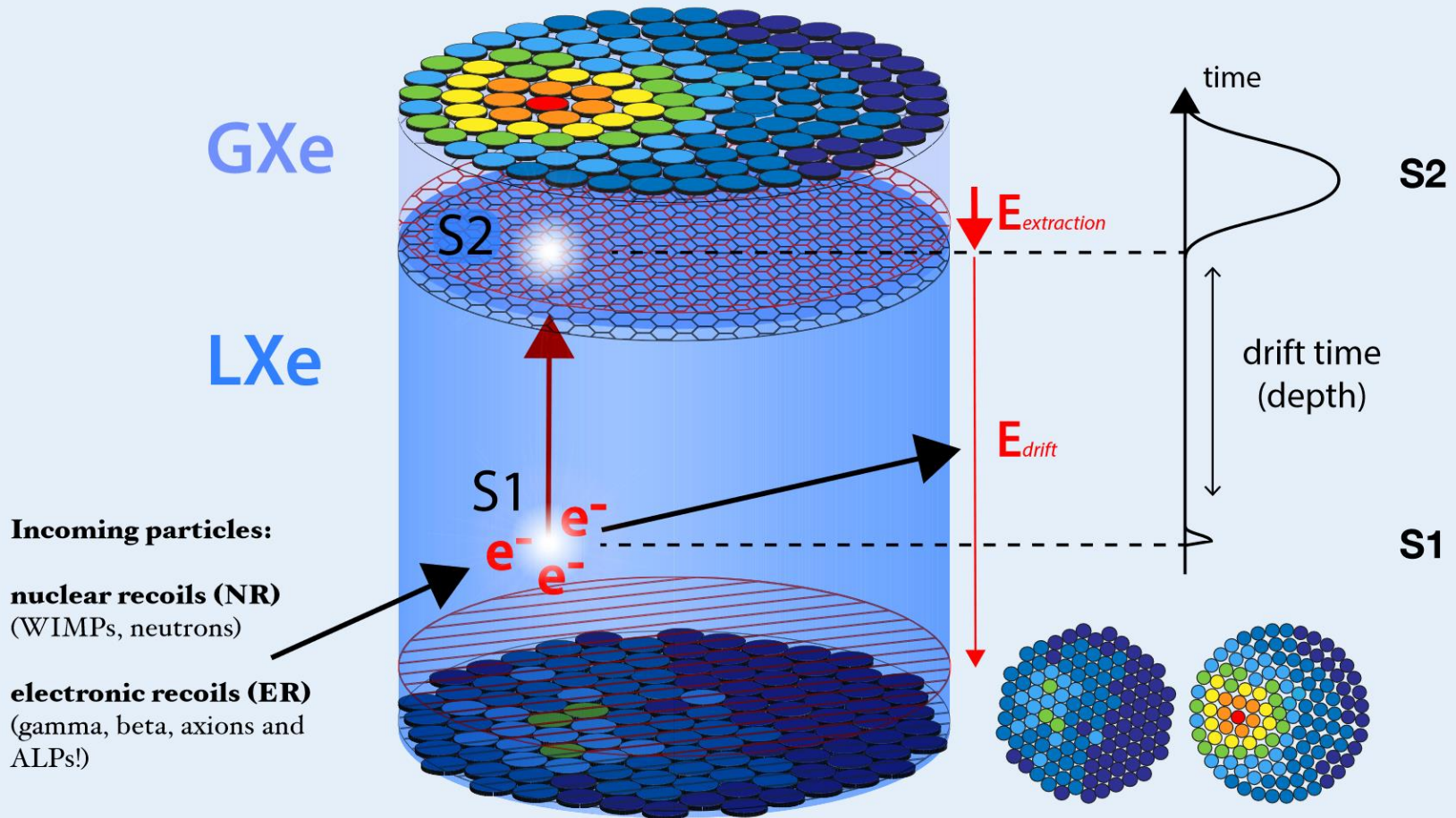
- ❑ For DM direct detection experiments, CRDM is an irreducible subcomponent of the Galactic DM
- ❑ CRDM do not suffer from the threshold problem, allowing for constraining ultra-light DM particles.
- ❑ For DM-nucleon scatterings, the nuclear formfactor suppresses the Earth attenuation of CRDM, making the Earth more transparent and enlarge the exclusion region of the cross section.
- ❑ The morphology of the CRDM is different from most of the other boost DM models, such a difference can be measured by future experiments such as hpyer-K

**Thanks for your attention !**

---

Backup slides

(LXe TPC)



Incoming particles:

**nuclear recoils (NR)**  
(WIMPs, neutrons)

**electronic recoils (ER)**  
(gamma, beta, axions and ALPs!)

GXe

LXe

S1

S2

S2

S1

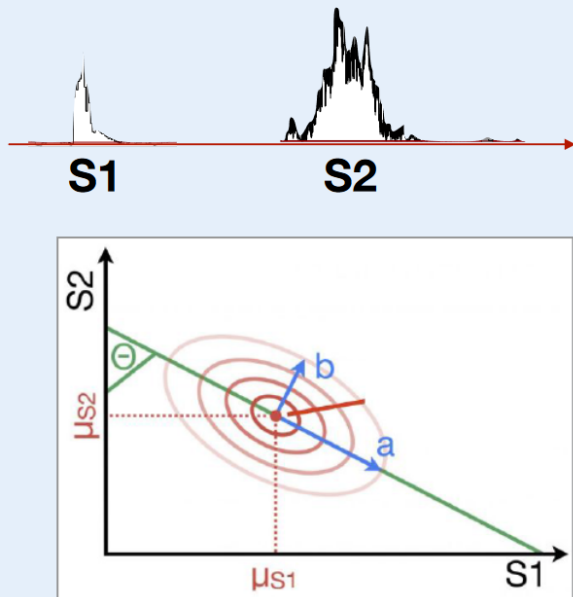
time

$E_{extraction}$

$E_{drift}$

drift time  
(depth)

# Energy reconstruction

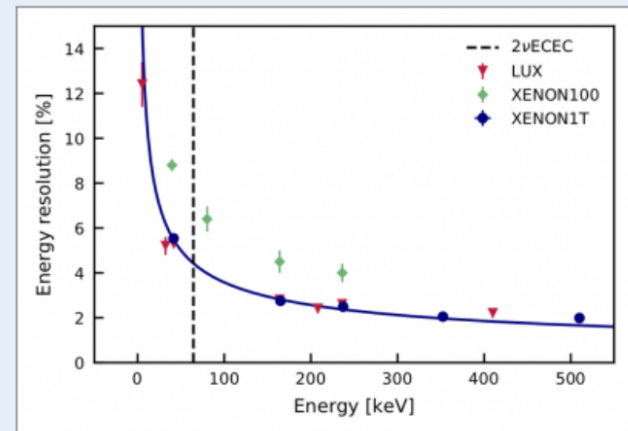
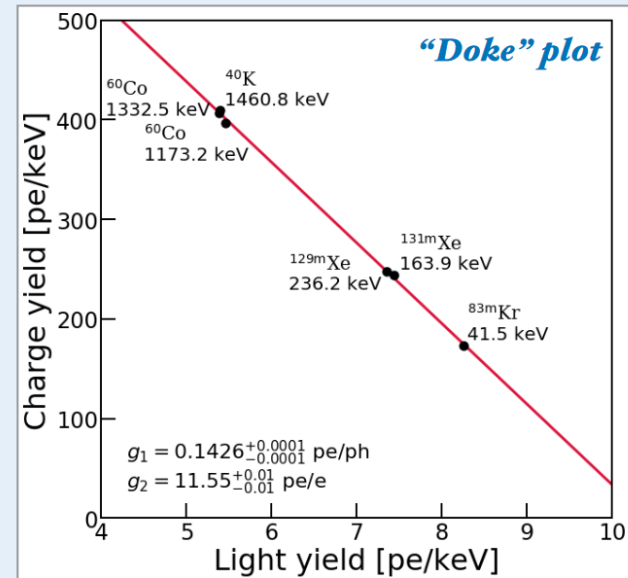


$$E = (N_{ph} + N_e) \cdot W = \left( \frac{S1}{g1} + \frac{S2}{g2} \right) \cdot W$$

where  $W = 13.7$  eV/quanta

$g_1$  and  $g_2$ : detector-specific gain constants  
 extract  $g_1/g_2$  from calibration data, use it to  
 reconstruct energy of each event

## Combined Energy Scale



Slide from Xenon-1T



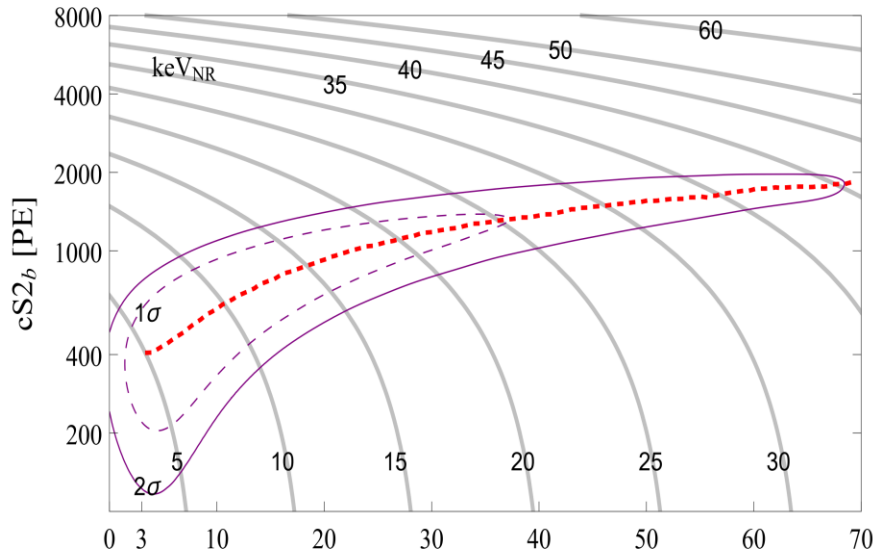
# Statistic approaches

## Statistic approaches

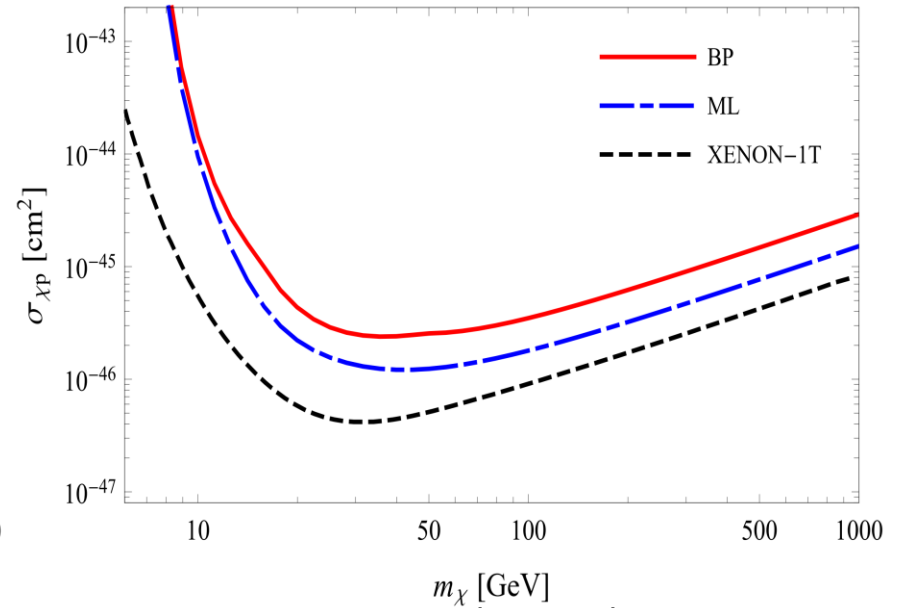
- ❑ Binned Poisson
- ❑ Maximal likelihood

$$1 - \alpha = (1 - \alpha_{\text{bin}})^{N_{\text{bin}}}$$

$$\text{TS} = -2 \ln \frac{\mathcal{L}(m_\chi, \sigma_{\chi p})}{\mathcal{L}(\hat{m}_\chi, \hat{\sigma}_{\chi p})}$$



MC simulation of halo DM signal  
( $m_\chi = ???$ )



Derived upper limits

# Go to indirect measurements of CR flux

Methods for measuring cosmic rays particles

- ❑ **direct: space based** calorimeters
  - Excellent mass resolution
  - Limited energy range, typically  $E < 200$  Tev (so far adopted by all the current analyses)
- ❑ **Indirect: ground based** air-shower arrays
  - Mass resolution limited to major groups
  - Very large energy range:  $E \sim 10^{20}$  eV,

